Isolating Small Extracellular Vesicles from Small Volumes of Blood Plasma using size exclusion chromatography and density gradient ultracentrifugation: A Comparative Study

Fang Kong[1,*], Megha Upadya[1], Andrew See Weng Wong[2], Rinkoo Dalan[3], Ming Dao[1,4,*]

1 School of Biological Sciences, Nanyang Technological University, SINGAPORE
2 Facility for Analysis, Characterisation, Testing and Simulation, Nanyang Technological University, SINGAPORE
3 Lee Kong Chian School of Medicine, Nanyang Technological University, SINGAPORE
4 Department of Material Science and Engineering, Massachusetts Institute of Technology, USA
*Author for correspondence: kongfang@ntu.edu.sg (K.F.); mingdao@mit.edu (M.D.)

Abstract:

Small extracellular vesicles (sEVs) are heterogeneous biological vesicles released by cells under both physiological and pathological conditions. Due to their potential as valuable diagnostic and prognostic biomarkers in human blood, there is a pressing need to develop effective methods for isolating high-purity sEVs from the complex milieu of blood plasma, which contains abundant plasma proteins and lipoproteins. Size exclusion chromatography (SEC) and density gradient ultracentrifugation (DGUC) are two commonly employed isolation techniques that have shown promise in addressing this challenge. In this study, we aimed to determine the optimal combination and sequence of SEC and DGUC for isolating sEVs from small plasma volumes, in order to enhance both the efficiency and purity of the resulting isolates. To achieve this, we compared sEV isolation using two combinations: SEC-DGUC and DGUC-SEC, from unit volumes of 500 µl plasma. Both protocols successfully isolated high-purity sEVs; however, the SEC-DGUC combination yielded higher sEV protein and RNA content. We further characterized the isolated sEVs obtained from the SEC-DGUC protocol using flow cytometry and mass spectrometry to assess their quality and purity. In conclusion, the optimized SEC-DGUC protocol is efficient, highly reproducible, and well-suited for isolating high-purity sEVs from small blood volumes.

Introduction

In recent years, extracellular vesicles (EVs) have garnered significant scientific attention due to their potential as biomarkers and applications in targeted drug delivery[1]. These vesicles are secreted by all cell types and have been detected in various types of bodily fluids such as blood, urine, saliva, and feces[2]. Comprising a phospholipid bilayer with a composition similar to the cell of origin, EVs carry a diverse range of molecules, including proteins, nucleic acids, and lipids[3]. They play crucial roles in both normal physiological processes and pathological conditions.

EVs can be classified into three main subgroups based on their biogenesis: exosomes, microvesicles (MVs), and apoptotic bodies. Due to the challenges in distinguishing between exosomes and MVs smaller than 150 nm, which share similar size, density, and protein markers, they are collectively referred to as small extracellular vesicles (sEVs)[4]. These sEVs are of particular interest in the field of biomarker research and targeted drug delivery, given their ubiquitous presence and functional relevance in various biological processes.

Blood plasma sEVs provide valuable information for diagnosis, prognosis, and homeostasis. However, isolation of sEVs from plasma is hindered by two major constituents: plasma proteins and lipoproteins[5–7]. Contamination of these constituents in sEV isolates can affect the understanding of the role of sEVs as carriers of genetic information and protein antigens in human physiology and pathology. Numerous techniques, including differential ultracentrifugation (dUC), size exclusion chromatography (SEC), ultrafiltration, immunoaffinity isolation, and microfluidics[8], are used to isolate sEVs from plasma. SEC[9] and density gradient ultracentrifugation (DGUC) are particularly popular due to their unique advantages in isolating sEVs based on size and buoyant density, respectively. In many occasions involving human blood, such as routine blood tests, only a small volume of blood

53 (1~10 ml) is collected, which yields a limited amount of plasma (500 µl to 5 ml). To obtain
54 high-purity sEVs with a reasonable yield from this small volume of plasma, it is essential to
55 establish a repeatable and reliable isolation protocol. Additionally, the isolation method
56 should be simple, practical, and involve commonly available equipment to ensure ease of use.
57 To address this challenge, we explored the combination of SEC and DGUC, which has been
58 shown to lead to high-purity sEV isolates by effectively removing both lipoproteins and
59 plasma proteins[10–14]. However, the ideal sequence for these methods in isolating sEVs
60 from small volumes of plasma remains unclear. In this study, we compared the sequences of
61 SEC-DGUC and DGUC-SEC to determine the better option in terms of purity and yield. Our
62 study reinforces previous findings[12,15] on the efficacy of size exclusion chromatography
63 (SEC) in eliminating plasma proteins and high-density lipoproteins (HDLs), as well as the utility
64 of density gradient ultracentrifugation (DGUC) in distinguishing small extracellular vesicles
65 (sEVs) from lipoproteins.
66 We examined the performance of two protocols, SEC-DGUC and DGUC-SEC, in terms of sEV
67 purity and yield. Both methods produced high-purity sEVs, but the SEC-DGUC protocol
68 outperformed DGUC-SEC in terms of sEV protein and RNA yield.
69 In order to enhance the efficiency of the DGUC process, we optimized it using a tailored
70 density gradient in a 1.5 ml tube format and a fixed-angle rotor. This adjustment significantly
71 reduced the ultracentrifugation time to just 2 hours. Our optimized approach enabled the
72 harvesting of sEVs across an extensive density range (> 1.08 g/ml), achieving high-purity
73 isolation in a short span of 3 hours. This study thus offers an efficient protocol for sEV isolation
74 that combines optimal yield and high purity. Subsequently, we further characterized the
75 isolated sEVs using flow cytometry and mass spectrometry techniques. These additional
76 investigations provided further confirmation of the sEVs' purity and structural integrity.

77 In conclusion, our study highlights the superiority of the SEC-DGUC protocol over DGUC-SEC
78 in terms of purity and yield when isolating sEVs from as little as 500 µL of plasma. This
79 optimized protocol is well-suited for clinical applications requiring high-purity sEVs from small
80 blood volumes and is easily adaptable for various research and clinical settings due to its
81 simplicity, practicality, and use of commonly available equipment.

82 **Result**

83 **2.1 SEC isolated particles from plasma with 1% sEV content**

84 We first assessed the efficacy of SEC in isolating particles, particularly sEVs, from plasma
85 (Figure 1A). A volume of 500 µl plasma was loaded onto a SEC column with a maximum
86 loading capacity of 2 ml. We collected and pooled four fractions, fraction 7-10 (2 ml total
87 volume), as the "particle fraction" (PF) for each SEC run. This procedure is consistent with the
88 particle concentration profiles (Supplementary Figure 1A) and follows the SEC column
89 manual's guidelines. NTA measurement of these PFs, obtained from 10 blood plasma samples,
90 demonstrated particle concentrations ranging from $9.6x10^{8}$ to $5.5x10^{11}$ ml^{-1}.

91 Cryo-EM images of PFs isolated from the plasma of 5 healthy individuals were used to analyse
92 the content of the PFs (Figure 1B). We observed distinct sEVs characterized by bilayer
93 membranes, although they were outnumbered by a large number of lipoproteins (Figure 1B
94 and Supplementary Figure 1C). The average proportion of sEVs in the PFs was 1%. Notably,
95 HDLs (7-13 nm)[16] were observed quite sparingly in the cryo-images of PFs, suggesting a
96 substantially lower presence compared to the other particle populations. On the other hand,
97 the size of the lipoproteins in PF mainly comprised two populations centred at 20-25 nm and
98 40-50 nm, corresponding to the sizes of LDL and IDL/VLDL, respectively (Supplementary
99 Figure 1F).

100 Our data demonstrated that SEC effectively removed plasma proteins and HDLs. However,
101 sEVs constituted only 1% of the particles in the PFs, with the remaining 99% consisting of a
102 mixture of LDL, IDL/VLDL lipoproteins.

103

104 **2.2 DGUC density gradient design inside a 1.5ml Eppendorf tube**

105 Addressing the challenges associated with handling small volumes of plasma in DGUC requires
106 an optimized approach, ideally involving the use of a smaller tube format, such as a 1.5 ml

107 Eppendorf tube. For such optimization, it's critical to accurately identify the density zones of
108 sEVs and lipoproteins, including their overlapping regions, to ensure effective separation.
109 To fulfil this initial objective, a DGUC experiment was conducted using a swing-bucket in a
110 conventional 12 ml tube. The PF from SEC of 6 ml plasma served as the starting material,
111 ensuring ample substance for subsequent TEM analysis (Supplementary Figure 2, Materials
112 and methods). After the DGUC, the 12 ml tube was fractionated into 42 distinct fractions,
113 each of which underwent NTA, TEM, and density measurements. This enabled correlation of
114 the density profile with particle concentrations and TEM images, fostering an understanding
115 of how sEVs separate from lipoproteins within the established density gradient
116 (Supplementary Figure 2). The analysis delineated three discrete density zones. The first zone,
117 with densities less than 1.05 g/ml, was characterized by high particle counts and a
118 predominance of lipoproteins, yet devoid of sEVs. The second, a separation zone, spanning
119 from 1.05 g/ml to 1.08 g/ml, displayed a reduction in particle numbers, emergence of sEVs,
120 and a continued dominance of lipoproteins. The final zone, extending beyond 1.08 g/ml and
121 up to 1.2 g/ml, marked as the sEV zone, exhibited a further drop in particle counts, a sharp
122 decrease in lipoproteins, and a marked increase in the presence of sEVs.
123 Building on the findings from the 12 ml tube format experiment, we aimed to establish a
124 density gradient within a more compact, 1.5 ml tube. This was accomplished by layering an
125 800 µl 10% iodixanol solution over a 20 µl 50% iodixanol cushion (Figure 2A). Subsequently,
126 the assembled density gradient was calibrated with an additional 500 µl of PBS followed by
127 DGUC, utilizing a fixed-angle rotor for durations of 2, 6, and 16 hours (see Materials and
128 methods).
129 Following the small-tube format DGUC, the tube was fractionated into 13 parts of 100 µl each,
130 with the first fraction at 120 µl to include the 20 µl 50% iodixanol cushion (Figure 2A). The

131 density profiles displayed notable consistency across different runs at the tested time
132 intervals of 2, 6, and 16 hours (Figure 2B). As the ultracentrifugation duration increased, the
133 profiles evolved from a stepwise to a more continuous pattern. Within the 1.5 ml tube, the
134 potential separation zone (1.05~1.08 g/ml) slimmed down from a region of 700 µl to 500 µl
135 and 300 µl as the ultracentrifugation period extended from 2 to 6 and 16 hours, respectively.
136 Concurrently, the potential sEV zone (>1.08 g/ml) expanded from 120 µl during a 2-hour
137 ultracentrifugation to 220 µl for both 6 and 16 hours. These findings indicated that a 2-hour
138 ultracentrifugation period resulted in the broadest separation zone and the smallest sEV zone.
139 Given the insights gained from these experiments, it appears that optimizing the DGUC
140 process for a smaller, 1.5 ml tube format and initially setting the ultracentrifugation period at
141 2 hours could be effective for isolating sEVs.
142
143 **2.3 DGUC isolated sEVs with significant protein contamination**
144 Building upon these observations, the effectiveness of the 1.5ml tube format DGUC was
145 evaluated for direct sEV isolation from plasma. A 500µl plasma sample was subjected to the
146 2-hour DGUC protocol, with the tube subsequently divided into 13 fractions. Each fraction's
147 particle and protein concentrations were subsequently measured (Figure 3). The high-density
148 bottom fraction (>1.08 g/ml), which contained sEVs, was denoted as plasma-DGUC-1. The
149 particle and protein concentration profiles revealed that the plasma-DGUC-1 fraction
150 successfully eliminated the majority of proteins and a significant number of particles (Figure
151 3). However, despite the substantial protein removal, the protein concentration in plasma-
152 DGUC-1 remained relatively high at 7.7mg/ml. This indicates that while DGUC effectively
153 separates low-density particles from those of high density, but a considerable amount of
154 proteins still remains within the sEV density zone.

155

156 **2.4 SEC-DGUC protocol isolated high-purity sEVs**

157 Recognizing the unique advantages and drawbacks of SEC and DGUC, it became clear that a
158 strategic integration of these methods could potentially enhance the isolation of high-purity
159 sEVs from blood plasma. With this perspective, we adopted a combined SEC-DGUC method.
160 Specifically, we subjected PFs, obtained from SEC of a 500µl plasma sample, to the small-tube
161 format DGUC protocol (Figure 4A). The tube contents were systematically divided into 13
162 fractions, each of which was subjected to NTA, TEM, and density measurements. As expected,
163 fraction 1, comprising the bottom 120µl, showed a high density (1.10 g/ml) and was
164 populated with high-purity sEVs (Figure 5). Fractions 2 to 7, within the 1.05~1.08 g/ml density
165 zone, displayed sparse sEV presence amidst lipoproteins, while the remaining fractions (8-13)
166 were dominated by lipoproteins (Figure 5 and Supplementary Figure 3). Distinct NTA size
167 histograms for fraction 1 further highlighted its divergence from the remaining fractions,
168 which were overwhelmed by lipoproteins (Supplementary Figure 4B). As a result, fraction 1
169 was identified as the final sEV isolate derived from the plasma sample using the SEC-DGUC
170 protocol.

171

172 To further substantiate the purity of the sEV isolates obtained through SEC-DGUC protocol,
173 we embarked on measuring the total RNA content of the fractions and conducting western
174 blot analysis (see Materials and methods). For these experiments, we simplified the
175 fractionation of the 1.5 ml tube into four distinct fractions, denoted as SEC-DGUC-1 to 4
176 (Figure 5 right side, see Materials and methods). Total RNA analysis revealed that SEC-DGUC-
177 1 had a higher concentration of RNA compared to the other three fractions (Figure 5). The
178 western blot analysis showed an abundant presence of sEV markers such as CD63, CD81, CD9,

179 TSG101, and Flotillin-1 in SEC-DGUC-1, while the lipoprotein marker, ApoB, was notably low.
180 This contrasted with SEC-DGUC-2 to 4, where ApoB was abundant, reinforcing the high purity
181 of sEVs in SEC-DGUC-1. Notably, SEC-PF exhibited a high level of ApoB and low expression of
182 sEV markers (Figure 6B).
183 To quantify the purity of sEVs in SEC-DGUC-1, cryo-EM was employed to discern sEVs and
184 lipoproteins (Figure 6D, Supplementary Figure 5). The purity of sEVs, defined as the
185 percentage of sEVs among all particles, was calculated to be 40%, where other 60% particles
186 were mainly small lipoproteins. Considering that SEC-PFs were comprised of only ~1% of sEVs,
187 the DGUC managed to eliminate over 98% of the lipoproteins.
188 Interestingly, when the ultracentrifugation time was increased to 16 hours, the size histogram
189 and particle concentration profile closely mirrored those of the 2-hour DGUC (Supplementary
190 Figure 4C-E). This observation suggests that a 2-hour DGUC was sufficient to separate sEVs
191 from lipoproteins in the 1.5 ml tube using the fixed-angle rotor.
192 In conclusion, the SEC-DGUC protocol successfully isolated sEVs from a small volume of
193 plasma under three hours in total by leveraging the strengths of SEC and DGUC.
194 **2.5 DGUC-SEC protocol also isolated high-purity sEVs**
195 An alternative approach to the sequential SEC-DGUC process involves reversing the order,
196 implementing DGUC prior to SEC (termed DGUC-SEC)[13,17]. DGUC separates high-density
197 particles from low-density ones in the plasma, while SEC further differentiates proteins and
198 HDL from sEVs. Theoretically, the DGUC-SEC protocol should also effectively isolate sEVs from
199 plasma. However, it remains intriguing to assess if the sequence of applying SEC and DGUC
200 impacts the quality of sEV isolates from a small volume of plasma.
201 For this purpose, 500 µl of plasma was initially processed through a 2-hour DGUC protocol
202 using the 1.5 ml tube format. The bottom 120 µl high-density fraction (plasma-DGUC-1) was

203 then collected and subjected to SEC (Materials and methods). Similar to the SEC-DGUC
204 protocol, this DGUC-SEC protocol also yielded a high-purity sEV isolate, termed DGUC-SEC-PF,
205 as confirmed by Western blot and transmission electron microscopy (TEM) (Figure 7A, D).

206 **2.6 Comparison of SEC-DGUC and DGUC-SEC protocols: SEC-DGUC obtained higher yield of**
207 **sEVs**

208 A side-by-side comparison of sEV isolates from the same plasma source using SEC-DGUC and
209 DGUC-SEC was carried out using western blot, TEM and total RNA analysis (Figure 7, see
210 Materials and methods). In the western blot, an additional sEV sample isolated by a routine
211 dUC protocol was included for comparison. Both sEV samples isolated by the combination of
212 SEC and DGUC using the same amount of plasma showed low contaminants (Calnexin,
213 Albumin, ApoA, and ApoB) and clear signal of sEV markers such as CD9, CD63, CD81, and
214 TSG101 (Figure 7A). In stark contrast, sEV isolated by dUC showed a high degree of
215 contamination of Albumin, ApoA, and ApoB, but also an abundance of CD9, CD81, and TSG101.
216 TEM images demonstrated similar appearances of the particles isolated by the two protocols.
217 The particle size distributions of isolated sEVs obtained from the TEM images by both SEC-
218 DGUC and DGUC-SEC protocols also largely overlapped with each other (Figure 7B), further
219 suggesting that the particles isolated by both protocols are similar both in chemical but also
220 in physical aspect. Despite the similarity of SEC-DGUC-1 and DGUC-SEC-PF samples, the SEC-
221 DGUC-1 did show higher signal intensity for all markers compared to the DGUC-SEC-PF in
222 western blot. In addition, the total RNA analysis (Figure 7E, F) showed that SEC-DGUC-1
223 contained more than 4 times the total amount of RNA than DGUC-SEC-PF, suggesting that the
224 SEC-DGUC protocol yielded significantly more sEVs.

225 In conclusion, both the SEC-DGUC and DGUC-SEC protocols proved effective in isolating high-
226 purity sEVs from plasma. Yet, in the context of our experiment, which aimed to isolate sEVs

227 from low plasma volumes, the SEC-DGUC protocol outperformed DGUC-SEC, yielding a
228 significantly greater quantity of sEVs.

229 **2.7 High purity of sEVs facilitate downstream analyses**

230 Building upon the results of the comparative analyses, we further examined the sEVs isolated
231 by SEC-DGUC through additional downstream analyses—surface marker detection by flow
232 cytometry (FCM) and protein content analysis by liquid chromatography with tandem mass
233 spectrometry (LC-MS/MS).

234 The sEV surface proteins were analyzed by FCM using a commercial kit such as the MACSPlex
235 Exosome kit, in a semi-quantitative manner (Figure 8A and B, see Materials and methods). A
236 panel of 37 surface markers comprehensively evaluated the sEVs in the plasma concerning
237 their origin and relative amount.

238 We compared the surface marker signals of SEC-DGUC-1 with SEC-PF (Figure 8C), derived from
239 the same plasma source, using the same amount of particles ($5x10^8$, calculated from the NTA
240 data), which was reported to be a saturating number[18]. The surface marker panel
241 demonstrated striking differences in signal strength between SEC-DGUC-1 and SEC-PF. For
242 some highly expressed surface markers, such as CD42a, CD41b, and CD29, the signals of SEC-
243 DGUC-1 were up to three orders of magnitude higher than SEC-PF (Figure 8C). Moreover, for
244 other surface markers such as CD3, CD19, HLAs, CD44, CD45, CD31, and SSEA-4, SEC-DGUC-1
245 provided much higher signals than the background, compared to SEC-PF, which showed
246 undetectable levels of signals. sEV isolates from two more different plasma exhibited a similar
247 trend (Supplementary Figure 6). The contrast between signals from SEC-DGUC-1 and SEC-PF
248 further confirmed the high purity of sEVs in SEC-DGUC-1 and suggested that high-purity sEV
249 isolates would lead to higher sensitivity in the FCM analysis.

250

251 Another crucial question to address is whether the sEVs isolated by SEC-DGUC represent the
252 sEV population in the original plasma. To investigate this, we compared the signal patterns of
253 the 37 surface markers across plasma, SEC-PF, SEC-DGUC-1, and sEVs isolated by dUC (Figure
254 8D). The signal pattern was calculated by normalizing individual surface marker signals to their
255 corresponding signal sum. The number of particles loaded for plasma, SEC-PF, SEC-DGUC-1,
256 and sEV isolated by dUC were $1x10^{10}$, $1x10^{10}$, $5x10^{8}$, and $5x10^{8}$ (based on NTA measurement),
257 respectively. The number of particles loaded for plasma and SEC-PF was 20 times more than
258 SEC-DGUC-1 to achieve a comparable level of sEV loading. The surface marker signal patterns
259 of SEC-PF and SEC-DGUC-1 were similar to plasma, whereas sEVs from dUC deviated from the
260 plasma (Figure 8D). This suggested that the sEVs isolated by the SEC-DGUC protocol
261 represented the sEV population in plasma, whereas sEVs isolated by dUC represented a
262 biased population.
263 In summary, SEC-DGUC-1 significantly improved the sensitivity of surface marker detection
264 compared to SEC-PF in flow cytometry, and the sEVs in SEC-DGUC-1 were found to be
265 representative of the sEV population in the original plasma.
266 Next, the SEC-PF and SEC-DGUC-1 obtained from 5 ml of a single plasma source were analyzed
267 by LC-MS/MS (Material and Methods). 343 proteins were identified in SEC-PF, and 754
268 proteins were identified in SEC-DGUC-1. Out of the 754 proteins identified in SEC-DGUC-1, 51
269 proteins matched with the top 100 sEV proteins from Vesiclepedia. Specific sEV-associated
270 proteins such as CD81, CD9, and TSG101 were identified. Additionally, other common EV-
271 associated proteins such as 14-3-3 protein (theta, zeta/delta), Rabs (Rab-7A and Rab-8A),
272 ADAM10, EHD4, PFN1, immune system-related proteins (MHC Class II), MSN, SDCBP, ENO1,
273 Annexin, GAPDH, ACTN4, TUBA1C, and ESCRT accessory (Clathrin) were also identified. The
274 following cell-specific markers were detected: CD41, CD36, CD42b for platelets; CD37 for

275 leukocytes, and CD163 for macrophages. Regarding the co-isolated contaminating
276 lipoproteins in the sEV isolate, only ApoA was detected in the top 50 most abundant proteins
277 according to emPAI (Supplementary Table I), which was expected based on the western blot
278 result (Figure 6B). On the other hand, for SEC-PF, 7 out of the top 11 most abundant proteins
279 were lipoproteins (Supplementary Table II). The identified proteins were further analysed
280 with the functional annotation tool on the platform of the Database for Annotation,
281 Visualization, and Integrated Discovery (DAVID v6.842), of which the top 10 in the functional
282 annotation chart were shown in Figure 9. Extracellular exosome was the top first group for
283 SEC-DGUC-1 (Figure 9A), suggesting the identified proteins were highly associated with sEVs.
284 In comparison, the top 3 annotation functions of proteins identified in SEC-PF were not
285 related to sEVs (Figure 9B).
286 In summary, sEVs isolated from a small volume of plasma using the SEC-DGUC protocol can
287 provide the required purity to identify sEV-associated proteins in mass spectrometry.
288
289 **2.8 Repeatability and reliability of the SEC-DGUC protocol**
290 We subsequently assessed the repeatability and reliability of the SEC-DGUC protocol in sEV
291 isolation from plasma, critically analysing variations at each step of the protocol.
292 The repeatability of the SEC step was examined using multiple SEC-PFs derived from the same
293 plasma source. Comparisons were based on particle concentration and size distribution (via
294 NTA) once concentrated to 500 µl. This test, utilizing six distinct plasma sources, revealed that
295 the coefficient of variation (CV) in particle concentration ranged between 6% and 55%
296 (Supplementary Figure 7 table). Meanwhile, size distributions exhibited no notable variations
297 across plasma samples (Supplementary Figure 7A-C), implying that despite potential
298 variations in particle numbers, the particle populations remained largely consistent across PFs.

299 The complete SEC-DGUC protocol was then scrutinized for its repeatability using multiple sEV
300 isolates (SEC-DGUC-1) from the same plasma source. Particle concentrations and size
301 distributions were evaluated, yielding CVs of 24% and 25% for particle concentration in SEC-
302 DGUC-1 (Supplementary Figure 8 table). The substantial overlap in size distributions for each
303 plasma (Figure 10B, Supplementary Figure 8) suggests a consistent population of isolated
304 particles.
305 The repeatability of the SEC-DGUC protocol was further evidenced by its consistent particle
306 concentration profile across the 1.5 ml tube. Four technical replicates of the profiles showed
307 good repeatability (Figure 10A), suggesting the SEC-DGUC protocol's ability to robustly
308 generate a consistent density gradient profile and particle subpopulations. Additionally, NTA-
309 measured size distributions displayed well-overlapped histograms of particles (Figure 10B),
310 reinforcing the protocol's robustness.
311 In the subsequent phase, we gauged the protocol's reliability across various plasma samples
312 by evaluating particle concentration profiles, size distributions, and TEM images of SEC-DGUC-
313 1. Particle concentration profiles derived from diverse plasma samples displayed a signature
314 'tick' shape, indicative of reliable sEV and lipoprotein separation irrespective of the plasma
315 source (Supplementary Figure 9). However, the size distributions of SEC-DGUC-1 varied across
316 different plasma samples (Supplementary Figure 10), suggesting that the characteristics of
317 sEVs were plasma-specific. TEM images of SEC-DGUC-1 derived from five different biobanked
318 plasma samples further confirmed the high purity of sEVs, with many particles exhibiting the
319 characteristic cup-shape and a low contrast (Figure 11).
320 In conclusion, the SEC-DGUC protocol demonstrated a CV of ~25% for particle number
321 repeatability when isolating sEVs from the same plasma source. Despite this, it exhibited a
322 reliable capacity to isolate high-purity sEVs from varying plasma sources.

323 **Discussion**

324 The task of isolating small extracellular vesicles (sEVs) from human plasma becomes
325 particularly challenging when dealing with minimal volumes. To tackle this challenge, our
326 study scrutinized two commonly employed methods –SEC and DGUC, and further investigated
327 the efficiency of their combined use. We found that neither SEC nor DGUC, when used
328 individually, provide an optimal solution for sEV isolation. SEC, although effective in removing
329 plasma proteins, results in a particle fraction dominated by lipoproteins (99%). DGUC, on the
330 other hand, facilitates substantial particle and protein removal due to its density-based
331 separation; however, it does not completely eliminate protein contamination.

332 The joint use of these methods has been explored previously, yet for small plasma volumes,
333 understanding how to strategically integrate these techniques to maximize efficiency and sEV
334 purity is crucial. Our devised SEC-DGUC protocol merges the advantages of both techniques,
335 employing SEC to eliminate plasma proteins and high-density lipoproteins (HDL), and DGUC
336 to remove remaining lipoproteins.

337 Interestingly, our results showed that performing SEC prior to DGUC yields a higher yield of
338 sEVs, especially for plasma volumes ranging from 500µl to 2ml. The gel matrix of the SEC
339 column tends to retain a portion of proteins and particles, causing sample loss. When a low
340 particle concentration sample is processed through an SEC column, this loss becomes more
341 significant. Consequently, performing SEC first—when sEVs, lipoproteins, and plasma
342 proteins are all present—distributes the loss among all components. Given the minor
343 proportion of sEVs in plasma, the loss is more likely absorbed by lipoproteins and plasma
344 proteins. Conversely, protocols that use SEC in the final isolation step could experience a
345 significant loss of sEVs, as most lipoproteins and plasma proteins have already been
346 removed[11]. Such protocols may yield a lower amount of sEVs or require a larger plasma

347 volume to obtain enough sEVs for subsequent analyses[11,13]. This could explain the lower
348 yield of sEVs observed in the DGUC-SEC protocol compared to the SEC-DGUC protocol.
349 The SEC-DGUC strategy has been adopted by others and has shown reliable results[12].
350 However, DGUC is typically performed in tubes of larger volume capacity, such as 12 ml[12]
351 or 16.8 ml[13] placed in swinging-bucket rotors. For our SEC-DGUC protocol, the DGUC was
352 carried out in a 1.5 ml tube format and the density gradient setup was designed to harvest all
353 sEVs with a density greater than 1.08 g/ml, rather than in a specified narrow range of density.
354 From our experiments, we recognized that small tubes are easier to handle, require shorter
355 handling time as well as lower volumes of reagents, are more suitable for benchtop
356 ultracentrifuges, and the fractions can be harvested manually without the need of specialized
357 equipment. More importantly, DGUC with the small-tube format is done using a fixed-angle
358 rotor which has a shorter sedimentation path length. This requires a much shorter time to
359 isolate sEVs (< 3 hours) compared to a larger volume tube format using a swinging-bucket
360 rotor which typically lasts ~ 16 hours or more. Moreover, DGUC using the small-tube format
361 resulted in high-purity sEV isolates collected in a volume of 120 µl, the concentration of which
362 enabled direct downstream analyses such as electron microscopy, western blot, total RNA
363 analysis and a multiplex bead-based flow cytometric assay.
364 The advantage of high-purity sEV isolates was demonstrated by flow cytometry and mass
365 spectrometry. Flow cytometry result demonstrated that the sEVs isolated by SEC-DGUC gave
366 a signal 3 orders of magnitude higher than using SEC alone, thereby improving the sensitivity
367 of the assay to a greater extent. Moreover, the surface marker pattern of 37 proteins helps
368 to assess the nature of the sEV isolates. The surface marker patterns matched closely among
369 the sEVs isolated from SEC-DGUC, SEC alone and the original plasma, suggesting a close
370 representation of sEVs isolated from SEC-DGUC to the original plasma. It is important to note

371 that, the surface marker patterns of sEVs isolated from a routine dUC protocol deviated
372 significantly from sEV populations in the original plasma.
373 There have been several studies using mass spectrometry to determine the proteome of
374 plasma-derived EVs[13,19–21]. Karimi et al. 2018 analysed sEVs isolated by a DGUC-SEC
375 protocol from large volumes of pooled healthy human plasma with LC-MS/MS and identified
376 1187 proteins. Many proteins identified were sEV-associated proteins such as CD63, CD9 and
377 CD81 and the identified proteins were closely associated with extracellular exosomes. In
378 comparison, when analysing the sEVs isolated by the newly introduced SEC-DGUC protocol
379 using 5 ml plasma from a single healthy individual, the proteomics data identified 753 proteins
380 which included sEV-specific proteins, such as CD81, CD9, Flotillin and TSG101. Moreover, the
381 proteins were closely associated with extracellular exosomes as well. We expect that, with a
382 better optimized LC-MS/MS protocol, the volume of plasma required for the sEV isolation can
383 be further reduced. Therefore, we conclude that the sEVs isolate obtained from the small
384 volume plasma SEC and DGUC protocol is of sufficient yield and purity for mass spectrometry
385 analysis.
386 The key to the consistency of the SEC-DGUC protocol lies in three aspects: first, the capability
387 of SEC to efficiently remove plasma proteins and HDL; second, the capacity of DGUC to
388 separate sEVs from low density lipoproteins; third, the careful manual handling during DGUC,
389 especially in the final step of harvesting the sEVs from the tube. When evaluated individually,
390 SEC is a well-established and quick method which is commercially available; DGUC with the
391 simple density gradient design enables consistency, precision and the potential to fully
392 automate the protocol thereby mitigating human error. For these reasons, the SEC-DGUC
393 protocol can be extrapolated to obtain high-purity sEVs in a repeatable and reliable manner.

394 Collectively, our results clearly demonstrated the quality of the isolated sEVs and the
395 robustness of SEC-DGUC protocol in a small-tube format. This is not to claim that the existing
396 protocols are less reliable than the currently developed protocol. In fact, there is room to
397 further improve the protocol in future efforts.

398 The SEC-DGUC protocol, though efficient, has limitations like potential damage to or
399 aggregation of sEVs[22], and low-level contamination with HDL. The iodixanol reagent
400 introduced in DGUC could potentially interfere with certain downstream analyses, and
401 variations in plasma samples might impact sEV purity. Although the protocol effectively
402 isolates representative sEVs from plasma, some lower density sEVs that require a longer
403 centrifugation time may be missed.

404 Isolating high-purity sEVs from small volumes of plasma is essential in fully realizing the
405 potential of using sEVs as biomarkers. It is of particular importance to standardize the sEV
406 isolation protocol so that the data obtained by different labs can be compared and integrated
407 with high confidence. The SEC-DGUC protocol presented here is relatively short, easy to carry
408 out, and isolates sEVs with high purity in a repeatable and reliable manner. The SEC-DGUC
409 protocol can be quickly adapted by any laboratory and can aid clinical studies that have
410 limited accessible plasma volumes. It potentially offers a pathway for the standardization of
411 sEV isolation from plasma.

412

413 **4. Materials and methods**

414 **Blood collection and preparation of platelet-free plasma**

415 The plasma used in this study was obtained from two sources, fresh blood and biobanked
416 plasma. Fresh blood was obtained with written informed consent from healthy adult males
417 aged between 25~45 years. All blood was collected after overnight fasting unless specified
418 otherwise in the figure legend. The volunteers were free of medications for at least 3
419 weeks. Blood was drawn in the morning using venepuncture technique with a 21G butterfly
420 needle into anticoagulant citrate dextrose-A (ACD-A) containing vacuette tubes (455055,
421 Greiner, Austria). Three vacuette tubes (each 9 *ml* volume) of blood was collected from each
422 volunteer. The vacuette tubes were inverted a few times to mix the blood with the
423 anticoagulant, placed in an upright position and processed within 20 minutes of collection.
424 We applied the International Society on Thrombosis and Haemostasis (ISTH) protocol to
425 prepare the platelet-free plasma (PFP). Briefly, the blood was centrifuged at 2500 *g* for 15
426 min at room temperature using a table-top centrifuge (Z206A, Hermle Labortechnik GmbH,
427 Germany) to remove blood cells, resulting in platelet-poor plasma (PPP). The PPP was
428 transferred into a new tube and centrifuged once again at 2,500 *g* for 15 minutes, resulting
429 in PFP. The PFP was transferred into a new tube, homogenized by gentle inversion, split into
430 500 *µL* aliquots in 1.5 *mL* eppendorf tubes and stored at -80 °C until further use. The
431 biobanked plasma samples were obtained from healthy males following overnight fasting
432 with written informed consent. Briefly, the blood was collected using venepuncture
433 technique with a 21G butterfly needle into ethylenediaminetetraacetic acid (EDTA) containing
434 vacuette tubes. The blood was then centrifuged at 1200 *g* for 15 min at 4°C with brake-two
435 in a horizontal swing-bucket centrifuge. The plasma fraction was collected within 0.1 *ml* of
436 the interphase with the buffy coat layer. The plasma was split in 500 *µl* aliquots in 1.5 *ml*

437 eppendorf tubes and stored at -80 °C until further use. All data shown in this paper used ACD-
438 A plasma unless indicated otherwise in the figure legends.
439
440 **Size exclusion chromatography**
441 An aliquot of frozen plasma was taken from –80 °C and allowed to thaw completely at room
442 temperature. SEC elution was performed using PURE-EVs SEC columns (HBM-PEV,
443 HansaBioMed Life Sciences, Tallinn, Estonia) following the manufacturer's protocol. Briefly,
444 the SEC columns were equilibrated to room temperature and washed with 3 x 10 *ml* particle-
445 free 1X phosphate buffer saline (PBS) (SH30256.01, Hyclone, UT, USA) to eliminate
446 preservative buffer residues. A volume of 500 *µL* of PFP was applied on top of each column.
447 Once the sample was inside the gel matrix, the column was loaded with particle-free 1 X PBS
448 (the mobile phase of the SEC column). The column was not allowed to dry out during this
449 process. Each of the fifteen fractions of 500 *µl* volume was collected, after which the column
450 was washed with approximately 20 *ml* of 1 X PBS and stored at 4°C. These SEC columns were
451 washed and reused up to 5 times.
452
453 The first six SEC fractions (3 *ml*) constituted void volume, hence were discarded and the rest
454 of the nine fractions were analysed for particle numbers and protein concentration. Fractions
455 7 to 10 which were subsequently identified as the particle fractions (PF) were pooled to a
456 volume of 2 *ml* and concentrated using an Amicon Ultra 100 kDa centrifugal filter (Merck
457 Millipore, MA, USA), made from regenerated cellulose, to a final volume of 500 *µl*.
458
459 **Density gradient ultracentrifugation**

460 To prepare the density solutions, a 50% Working Solution was firstly made by diluting 5 vol of
461 iodixanol (Optiprep™, D1556, Sigma Aldrich, MO, USA) with 1 vol of 0.25 *M* Sucrose, 6 *mM*
462 EDTA, 60 *mM* Tris-HCl (pH 7.4). The Working Solution was then mixed with Homogenization
463 Medium composed of 0.25 M sucrose, 1 *mM* EDTA, and 10 *mM* Tris-HCl, (pH 7.4) to prepare
464 density solutions of desired percentages.
465
466 For DGUC experiment using the 12 *ml* tube, PFs obtained from 6 *ml* of plasma (24 *ml* total
467 volume as previously described) were concentrated to 6 *ml* and added to a Beckman Coulter
468 ultra-clear centrifuge tube (344059, Beckman Coulter, USA). A density gradient was carefully
469 constructed by underlying 2 *ml* each of 10%, 30%, and 50% iodixanol cushions sequentially.
470 The gradient tube was balanced and subjected to ultracentrifugation at 150,000 x *g* for 2 *h* at
471 4 °*C* using a swinging-bucket rotor (SW 41 Ti Beckman Coulter, USA).
472
473 For the DGUC using the 1.5 *ml* tube format, 500 *µl* of the concentrated PF obtained from a
474 single SEC (as previously described) was added to a Beckman Coulter ultracentrifuge tube
475 (357448, Beckman Coulter, USA). For plasma volume higher than 500 *µl*, SEC-PFs from
476 multiple SECs were pooled and concentrated to 500 *µl* before adding to the ultracentrifuge
477 tube. A density gradient was carefully constructed by underlying 800 *µl* of 10% iodixanol
478 solution and 20 *µl* of 50% iodixanol sequentially. The gradient tubes were balanced and
479 subjected to centrifugation at 135,000 x *g* for 2 *h* at 4 °*C* using a fixed-angle rotor (TLA-55,
480 Beckman Coulter, USA). After DGUC, thirteen fractions starting from the bottom of the tube
481 were manually collected by using gel loading pipetting tips. In total RNA analysis and western
482 blot experiments, fractions 2-4; 5-10 and 11-13 were pooled together for easier analyses.
483 Thus, four main fractions were analysed namely: SEC-DGUC-1 (120 *µl* volume), SEC-DGUC-2

484 (2-4 pooled, 300 *µl* volume), SEC-DGUC-3 (5-10 pooled, 600 *µl* volume) and SEC-DGUC-4 (11-
485 13 pooled, 300 *µl* volume) (Figure 6A).
486
487 **DGUC-SEC**
488 For the DGUC-SEC protocol, 500 *µl* of plasma was added to Beckman Coulter centrifuge tubes
489 (357448, Beckman Coulter, USA) and followed by underlying 800 *µl* of 10% iodixanol solution
490 and 20 *µl* of 50% iodixanol sequentially. The gradient tubes were subjected to centrifugation
491 at 135,000 x *g* for 2 *h* at 4 *°C* using a fixed-angle rotor (TLA-55, Beckman Coulter, USA). After
492 DGUC, the bottom 120*µl* was collected as the high density fraction and designated as plasma-
493 DGUC-1. The plasma-DGUC-1 was then topped up to a volume of 500 *µl* with 1X PBS to run
494 through the SEC column. Fractions 7 to 10 from the SEC were collected, pooled together, and
495 concentrated to a final volume of 120 *µl* using an Amicon Ultra 100 kDa centrifugal filter
496 (Merck Millipore, MA, USA). For plasma volume higher than 500 *µl,* multiple tubes were
497 processed in parallel in the DGUC step, and the resulting plasma-DGUC-1 fractions were
498 pooled and subjected to SEC to obtain sEV isolates.
499
500 **Total protein analysis**
501 Protein contents of the SEC fractions were measured using a BCA protein assay kit (23225,
502 Pierce, Thermo Fisher Scientific, MA, USA). A standard curve (range 0–1000 *µg/ml*) was
503 derived with six points of serial dilution with bovine serum albumin (BSA). BSA standard or
504 samples (10 *µl*) were transferred to a 96-well plate (Thermo Scientific Nunc MicroWell) to
505 which 100 *µl* working reagent was added (working reagent 50:1 ratio of assay reagents A and
506 B). The plate was incubated for 30 min at 37°C before being analysed with a multi-well
507 spectrophotometer at 562 *nm* (Tecan Infinite M200Pro, Switzerland). The average 562 *nm*

508 absorbance measurement of the blank replicates was subtracted from all other individual
509 standard and unknown sample replicates. A standard curve was obtained from the
510 measurement of BSA standard. The protein concentration of each unknown sample was
511 calculated based on the standard curve.
512
513 **Density measurement**
514 The density of fractions obtained from DGUC was determined by absorbance spectroscopy
515 (Tecan Infinite M200Pro, Switzerland) reading at 340 *nm* in a flat-bottomed 96-well
516 polystyrene plate (167008 Nunclon, ThermoFisher Scientific, MA, USA). A range of iodixanol
517 solutions (5–50%) was diluted at a 1:1 ratio with deionized water and measured in the same
518 96-well plate to serve as the standard control. For iodixanol concentrations above 35%, a
519 second dilution of the solutions was done to avoid absorbance values above 1.2. Also included
520 were water and 0.25 *M* sucrose as blanks. Each sample was triplicated to reduce random error.
521 Prior to measuring the absorbance, the plate was shaken thoroughly to mix the samples. A
522 standard curve was prepared by plotting the predetermined densities[22] of the 2-50%
523 iodixanol solutions against their mean absorbance. Using the standard curve, the densities of
524 the fractions collected from the iodixanol gradient following DGUC were calculated.
525
526 **Nanoparticle tracking analysis**
527 Nanoparticle tracking analysis (NTA) was carried out using ZetaView® (PMX 120, Particle
528 Metrix, Meerbusch, Germany). Samples were diluted to the recommended particle
529 concentration with particle-free 1 X PBS prior to analysis. The particle motion was measured
530 over 11 positions with two repeats at each position with the following parameters, frame rate:

531 30 fps; number of frames recorded: 60; sensitivity: 80; exposure: 100; minimum brightness:
532 30; minimum pixel size: 10; maximum pixel size: 10000; trace length: 30; temperature: 25 °*C*.
533
534 **Western blotting**
535 In the first experiment (Figure 6B), SEC-PF and sEV isolates from 2 *ml* of plasma obtained by
536 SEC and SEC-DGUC respectively were analysed for the presence of sEV and lipoprotein
537 markers. The same loading volumes of 22 *µl* were used for SEC-DGUC-1 to 4. Since 500 *µl* SEC-
538 PF was loaded on top of 820 *µl* iodixanol in the 1.5 *ml* tube, resulting in a total volume of 1320
539 *µl*, the equivalent loading volume for SEC-PF was calculated to be 22 x 500/1320 = 8.3 *µl*. The
540 loading particle number (based on NTA measurement) of SEC-PF and SEC-DGUC-1 to 4 were
541 $1.8x10^{10}$, $8.8x10^{8}$, $5.9x10^{8}$, $5.5x10^{9}$, $2.86x10^{10}$, respectively. In this manner, not only the
542 amount of sEVs against lipoproteins of each fraction can be evaluated, but also the particle
543 concentration profile in the 1.5 *ml* tube after SEC-DGUC can be analysed.
544
545 In the second experiment (Figure 7A), SEC-PF and 3 sEV isolates obtained from 2 *ml* plasma
546 using SEC-DGUC, DGUC-SEC and dUC were examined for the presence of sEV and lipoprotein
547 markers. The sEVs from SEC-DGUC, DGUC-SEC and dUC were collected in a volume of 120 *µl*
548 and same loading volumes of 30 *µl* were used. The sample loading volume for SEC-PF (11.4
549 *µl)* was calculated as described above. All samples were lysed in radioimmunoprecipitation
550 assay (RIPA) buffer (89900, Pierce, Thermo Scientific, MA, USA) containing protease inhibitor
551 cocktail (36978, Thermo Scientific, MA, USA) while chilling on ice. After mixing with loading
552 buffer (4 x) containing β-mercaptoethanol (80570, Merck, Darmstadt, Germany) and heated
553 to 70 ˚*C* for 10 *min*, the samples were loaded on 12% SDS-PAGE gels and electrophoresed to
554 detect sEV markers CD63, CD9, CD81, Flotillin-1, TSG101 and lipoprotein markers ApoA-I and

555 ApoB. After been transferred to 0.45 *μm* nitrocellulose membranes (1620115, Bio-rad,
556 Feldkirchen, Germany), proteins were stained with REVERT total protein stain (926-11015, Li-
557 COR Biosciences, Lincoln, NE, USA) for normalisation. After this, membranes were blocked at
558 room temperature for 1 *h* with Odyssey blocking buffer TBS (927-50000, Li-COR Biosciences,
559 Lincoln, NE, USA), and incubated overnight at 4 *°C* with 1:1000 of the following antibodies:
560 mouse monoclonal anti-CD63 (MX-49. 129.5) (sc-5275, Santa Cruz Biotechnology, Dallas, TX,
561 USA), rabbit monoclonal (9EPR2949) anti-CD9 (ab92726, Abcam, Cambridge, MA, USA);
562 mouse monoclonal anti-CD81 (B-11) (sc-166029 Santa Cruz Biotechnology, Dallas, TX, USA),
563 rabbit polyclonal anti-Flotillin-1 (ab41927, Abcam, Cambridge, MA, USA), rabbit polyclonal
564 anti-TSG101 (ab30871, Abcam, Cambridge, MA, USA), mouse monoclonal anti-ApoA-I (B-10)
565 (sc-376818, Santa Cruz Biotechnology, Dallas, TX, USA), mouse monoclonal anti-ApoB (C1.4)
566 (sc-13538, Santa Cruz Biotechnology, Dallas, TX, USA), mouse monoclonal anti-Albumin
567 (ab10241 Abcam, Cambridge, MA, USA) and rabbit polyclonal anti-Calnexin (ab22595, Abcam,
568 Cambridge, MA, USA). The membranes were washed by TBS with 0.1% Tween 20 (TBS-T), and
569 incubated at room temperature for 1 *h* with IgG secondary antibodies at 1:15,000, i.e., IRDye
570 800CW anti-mouse (925-32210, Li-COR Biosciences, Lincoln, NE, USA) and IRDye 680LT anti-
571 rabbit (926-68021, Li-COR Biosciences, Lincoln, NE, USA). Membranes were washed again
572 with 1X TBS-T and scanned with an Odyssey CLx imaging system (Li-COR Biosciences) using
573 700 and 800 *nm* channels. Visualization was done by ImageStudio software version 5.2 (LI-
574 COR Biosciences).
575
576 **Transmission electron microscopy**
577 The transmission-electron microscopy experiments were carried out at Cryo-Electron
578 Microscopy Platform, NTU Institute of Structure Biology. A carbon-coated grid (CF300-CU,

579 Electron Microscopy Sciences, Hatfield, PA, USA) was glow-discharged for 1 *min* before
580 placing 4 *μl* sample for adsorption of 1 *min*. After blotting, the grid was negatively stained for
581 1 *min* using 4 *μl* of 2% uranyl acetate. The grid was then blotted and air-dried for TEM imaging.
582 Grids were imaged using a T12 transmission electron microscope operating at 120 *kV* with an
583 Eagle 4k HS camera. TEM images were analysed using ImageJ[23] with Nanodefine plug-in[24]
584 to identify and count particles. Particles with low contrast were difficult to recognize by the
585 Nanodefine plug-in and they were counted and measured manually using ImageJ measuring
586 tools.
587
588 **Cryo electron microscopy**
589 The cryo-electron microscopy experiments were carried out at Cryo-Electron Microscopy
590 Platform, NTU Institute of Structure Biology. SEC-PF and SEC-DGUC-1 samples that
591 demonstrated an NTA concentration of at least $3x10^{11}$ particles were selected for Cryo-EM
592 imaging. For SEC-DGUC-1, an additional step of dialysis using Pur-A-Lyzer™ Mini 6000 dialysis
593 kit (PURN60030, Sigma-Aldrich, MO, USA) was added to remove iodixanol before grid
594 preparation. The grid preparation protocol follows Wang et al. 2020[25]. Briefly, a volume of
595 2~3 *μl* of the sample was applied to a glow discharged Quantifoil R2/2 grid coated with 2 *nm*
596 carbon (Jena, Germany) and incubated for 5~10 *mins*. The grid was then loaded into FEI
597 vitrobot. Another 2 *μl* of the sample was added to the grid and immediately blotted with
598 following parameters, blotting time: 3 *s*; humidity: 100%; temperature: 4 *°C*; blotting force: -
599 1; waiting time: 0 *s*;. and thereafter grids were flash frozen in liquid N2-cooled liquid ethane.
600 Grids were imaged on an Arctica transmission electron microscope (FEI) operated at 200 *kV*
601 on a Falcon III (FEI) direct electron detector. The Cryo-EM images were analysed manually
602 using ImageJ.

603 **Total RNA isolation**

604 For total RNA isolation, 100 *µl* isolates obtained from 2 *ml* of plasma following the SEC-DGUC
605 (SEC-DGUC 1-4) and DGUC-SEC protocols were used. RNA extraction was done using the
606 miRNeasy Serum/Plasma Kit (217184, Qiagen, GmbH, Hilden, Germany) according to the
607 quick-start protocol by the manufacturer. Briefly, 500 *µL* of QIAzol lysis reagent (#79306) was
608 added to the isolates, mixed by pipetting, and incubated at room temperature (RT) for 5 min.
609 After adding 100 *µL* chloroform, the tubes were capped securely and shaken vigorously for 15
610 *s*. The tubes were then incubated for 3 *min* at RT and centrifuged at 12,000 *g* for 15 *min* at
611 4 *°C*. The upper aqueous phase (~300 *µl*), containing total RNA, was carefully transferred to
612 a new 2 *ml* collection tube without transferring any interphase. 1.5 volumes of 100% ethanol
613 were added (~450 *µl*), and the samples were mixed thoroughly by pipetting. Up to 700 *µl* of
614 sample was pipetted into Qiagen RNeasy MinElute spin column in a 2 *ml* collection tube, the
615 tubes were capped and centrifuged at 8000 *g* for 15 *s* at RT. The flow-through was discarded.
616 This step was repeated until all the sample passed through the spin column. 700 *µl* Buffer
617 RWT (Qiagen #1067933) was added to each column, then the tubes were capped and
618 centrifuged for 15 *s* at 8000 *g*, RT after which the flow-through was discarded. 500 *µl* Buffer
619 RPE (Qiagen #1018013) was added to each column, the tubes were capped and centrifuged
620 for 15 *s* at 8000 *g*, RT, then the flow-through was discarded. This step was repeated, but
621 during the second time, the tubes were centrifuged for 2 *min* instead. The spin column was
622 placed inside a new 2 *ml* RNAse-free collection tube and was centrifuged at full speed for 5
623 *min* at RT with the tube cap left open to dry the membrane. The collection tube containing
624 the flow-through was discarded. Finally, the spin column was placed into a 1.5 *ml* RNAse-free
625 collection tube, and 14 *µl* nuclease-free water was added directly to the centre of the column,
626 then centrifuged at full speed at RT for 1 *min* to elute the RNA. The eluate was run through

627 the column again to maximise the RNA recovery. The RNA was immediately placed on ice.
628 RNA profile and concentration was then assessed by 2100 Bioanalyzer using RNA 6000 Pico
629 kit (Agilent Technologies) according to manufacturer's protocol.
630
631 **sEV surface protein profiling by flow cytometry**
632 The MACSPlex Exosome kit (Miltenyi Biotec, Bergish Gladbach, Germany) utilizes beads
633 functionalized with 37 types of antibodies to capture sEVs expressing the corresponding
634 surface markers. The sEVs captured by the beads are then labelled with a cocktail of
635 fluorescent labelled CD9, CD63 and CD81 antibodies which are detected by FCM. The
636 expression of 37 surface markers (CD1c, CD2, CD3, CD4, CD8, CD9, CD11c, CD14, CD19, CD20,
637 CD24, CD25, CD29, CD31, CD40, CD41b, CD42a, CD44, CD45, CD49e, CD56, CD62P, CD63,
638 CD69, CD81, CD86, CD105, CD133, CD142, CD146, CD209, CD326, HLA-ABC, HLA-DRDPDQ,
639 MCSP, ROR1, and SSEA-4) was evaluated by flow cytometry (FCM) with the short protocol
640 specified by the manufacturer. Briefly, 5×10^{8} of particles/sample (calculated based on NTA
641 measurement) or PBS (negative control) were diluted with MACSPlex buffer into 1.5 *ml*
642 microcentrifuge tubes with a final volume of 120 *μl*. Each tube was incubated at room
643 temperature for 1 *h* in the dark with 10 *μl* of MACSPlex exosome capture beads and 15 *μl* of
644 the mix of APC-conjugated antibodies. Post-incubation, beads were washed twice with 500 *μl*
645 of MPB at 3000 *g* for 5 *min*. Each time of washing, the supernatant was aspirated, leaving a
646 residual volume of 150 *μl*. The prepared beads were then analysed by BD LSR Fortessa X-20
647 flow cytometer (BD Biosciences, San Jose, CA, USA). All mean fluorescence intensity (MFI) was
648 background corrected according to the negative control.
649

650 For FCM comparison of sEV populations among plasma, SEC, SEC-DGUC and dUC, 5×10^8 of
651 particles/sample were mixed with 15 *µl* of MACSPlex exosome capture beads and incubated
652 at room temperature for 1 hr in the dark. The beads were then washed thrice with 500 *µl* of
653 MPB at 3000 *g* for 5 *min*. 15 µl of the mix of APC-conjugated antibodies was added to each
654 sample and incubated at room temperature for 1 *h* in the dark. Post-incubation, beads were
655 washed thrice with 500 *µl* of MPB at 3000 g for 5 *min*. Each time of washing, the supernatant
656 was aspirated, leaving a residual volume of 150 µl. The prepared beads were then analysed
657 by BD LSR Fortessa X-20 flow cytometer as described above.
658
659 **sEV protein profiling by liquid chromatography with tandem mass spectrometry**
660 Mass spectrometry experiments were carried out at the proteomics core facility in the School
661 of Biological Science at Nanyang Technological University. For SEC-DGUC-1, which was
662 obtained from 5 *ml* of plasma, the first step was to remove the iodixanol through dialysis using
663 Pur-A-Lyzer™ Mini 6000 dialysis kit (PURN60030, Sigma-Aldrich, Co., STL, MO, USA). Then SEC-
664 DGUC-1 was subjected to in-solution digestion prior to fractionation on an Xbridge™ C18
665 column (4.6 × 250 *mm*, Waters, Milford, MA, USA) and subsequent analysis by LC-
666 MS/MS. SEC-PF was subjected to in-solution digestion and subsequent analysis by liquid
667 chromatography with tandem mass spectrometry (LC-MS/MS).
668
669 For LC-MS/MS procedure, the peptides were separated and analyzed using a Dionex Ultimate
670 3000 RSLCnano system coupled to a Q Exactive instrument (Thermo Fisher Scientific, MA,
671 USA). Separation was performed on a Dionex EASY-Spray 75 *µm* × 10 *cm* column packed with
672 PepMap C18 3 *µm*, 100 *Å* (Thermo Fisher Scientific) using solvent A (0.1% formic acid) and
673 solvent B (0.1% formic acid in 100% ACN) at a flow rate of 300 *nl/min* with a 60 *min* gradient.

674 Peptides were then analyzed on a Q Exactive apparatus with an EASY nanospray source
675 (Thermo Fisher Scientific) at an electrospray potential of 1.5 *kV*.
676
677 Raw data files were processed and searched using Proteome Discoverer 2.1 (Thermo Fisher
678 Scientific). The Mascot algorithm was then used for data searching to identify proteins using
679 the following parameters: missed cleavage of two; dynamic modifications were oxidation
680 (+15.995 Da) (M) and Phosphorylation (+79.966 Da) (S, T, Y). The static modification was
681 Carbamidomethyl (+57 Da) (C). Percolator was applied to filter out the false MS2 assignments
682 at a strict false discovery rate of 1 % and relaxed false discovery rate of 5%. Only proteins
683 identified with 2 or more peptides were included in the final list.
684
685 **Conflict of Interests**
686 The authors declare that they have no conflict of interests.
687
688 **Author Contributions**
689 Kong Fang and Megha Upadya planned, designed and performed the experiments. Kong Fang
690 and Megha Upadya performed the sEV isolation and characterization. Kong Fang and Andrew
691 See Weng Wong performed electron microscopy. Kong Fang, Megha Upadya and Rinkoo
692 Dalan collected blood samples. Ming Dao and Kong Fang initiated, designed and
693 conceptualized the study. Kong Fang, Megha Upadya and Ming Dao wrote the manuscript.
694
695 **Data Availability Statement**
696 All data needed to evaluate the conclusions in the paper are present in the paper and/or the
697 Supplementary Materials. Additional data related to this paper may be requested from the

698 authors. Experimental procedures have been uploaded to EV-TRACK[26] with reference no.
699 EV210379.
700
701 **Acknowledgement**
702 This research has been funded through Nanyang Technological University Distinguished
703 University Professorship awarded to S.S.. M.D. acknowledges partial support from National
704 Institutes of Health under Grant No. R01HL154150. We appreciate the guidance from Prof.
705 Bernhard Otto Boehm on the clinical aspects of sEV research. We thank Asst. Prof. Hou Han
706 Wei for use of the Zetaview facility. We would like to express gratitude to Tan Tock Seng
707 Hospital for providing the biobank samples.
708

709 **References**

710 1. Andaloussi, S.E.; Mäger, I.; Breakefield, X.O.; Wood, M.J.A. Extracellular Vesicles: Biology and
711 Emerging Therapeutic Opportunities. *Nat. Rev. Drug Discov.* **2013**, *12*, 347–357,
712 doi:10.1038/nrd3978.
713 2. Witwer, K.W.; Buzás, E.I.; Bemis, L.T.; Bora, A.; Lässer, C.; Lötvall, J.; Hoen, E.N.N.-'t; Piper,
714 M.G.; Sivaraman, S.; Skog, J.; et al. Standardization of Sample Collection, Isolation and Analysis
715 Methods in Extracellular Vesicle Research. *J. Extracell. Vesicles* **2013**, *2*, 20360,
716 doi:10.3402/jev.v2i0.20360.
717 3. Colombo, M.; Raposo, G.; Théry, C. Biogenesis, Secretion, and Intercellular Interactions of
718 Exosomes and Other Extracellular Vesicles. *Annu. Rev. Cell Dev. Biol.* **2014**, *30*, 255–289,
719 doi:10.1146/annurev-cellbio-101512-122326.
720 4. Witwer, K.W.; Théry, C. Extracellular Vesicles or Exosomes? On Primacy, Precision, and
721 Popularity Influencing a Choice of Nomenclature. *J. Extracell. Vesicles* **2019**, *8*, 1648167,
722 doi:10.1080/20013078.2019.1648167.
723 5. Simonsen, J.B. What Are We Looking At? Extracellular Vesicles, Lipoproteins, or Both? *Circ. Res.*
724 **2017**, *121*, 920–922, doi:10.1161/CIRCRESAHA.117.311767.
725 6. Muller, L.; Hong, C.-S.; Stolz, D.B.; Watkins, S.C.; Whiteside, T.L. Isolation of Biologically-Active
726 Exosomes from Human Plasma. *J. Immunol. Methods* **2014**, *411*, 55–65,
727 doi:10.1016/j.jim.2014.06.007.
728 7. van der Pol, E.; Sturk, A.; van Leeuwen, T.; Nieuwland, R.; Coumans, F.; ISTH-SSC-VB Working
729 group Standardization of Extracellular Vesicle Measurements by Flow Cytometry through
730 Vesicle Diameter Approximation. *J. Thromb. Haemost. JTH* **2018**, *16*, 1236–1245,
731 doi:10.1111/jth.14009.
732 8. Wu, M.; Ouyang, Y.; Wang, Z.; Zhang, R.; Huang, P.-H.; Chen, C.; Li, H.; Li, P.; Quinn, D.; Dao, M.;
733 et al. Isolation of Exosomes from Whole Blood by Integrating Acoustics and Microfluidics. *Proc.*
734 *Natl. Acad. Sci.* **2017**, *114*, 10584–10589, doi:10.1073/pnas.1709210114.
735 9. Böing, A.N.; van der Pol, E.; Grootemaat, A.E.; Coumans, F.A.W.; Sturk, A.; Nieuwland, R. Single-
736 Step Isolation of Extracellular Vesicles by Size-Exclusion Chromatography. *J. Extracell. Vesicles*
737 **2014**, *3*, doi:10.3402/jev.v3.23430.
738 10. Théry, C.; Amigorena, S.; Raposo, G.; Clayton, A. Isolation and Characterization of Exosomes
739 from Cell Culture Supernatants and Biological Fluids. *Curr. Protoc. Cell Biol.* **2006**, *Chapter 3*,
740 Unit 3.22, doi:10.1002/0471143030.cb0322s30.
741 11. Zhang, X.; Borg, E.G.F.; Liaci, A.M.; Vos, H.R.; Stoorvogel, W. A Novel Three Step Protocol to
742 Isolate Extracellular Vesicles from Plasma or Cell Culture Medium with Both High Yield and
743 Purity. *J. Extracell. Vesicles* **2020**, *9*, 1791450, doi:10.1080/20013078.2020.1791450.
744 12. Vergauwen, G.; Tulkens, J.; Pinheiro, C.; Cobos, F.A.; Dedeyne, S.; Scheerder, M.-A.D.;
745 Vandekerckhove, L.; Impens, F.; Miinalainen, I.; Braems, G.; et al. Robust Sequential Biophysical
746 Fractionation of Blood Plasma to Study Variations in the Biomolecular Landscape of
747 Systemically Circulating Extracellular Vesicles across Clinical Conditions. *J. Extracell. Vesicles*
748 **2021**, *10*, e12122, doi:10.1002/jev2.12122.
749 13. Karimi, N.; Cvjetkovic, A.; Jang, S.C.; Crescitelli, R.; Hosseinpour Feizi, M.A.; Nieuwland, R.;
750 Lötvall, J.; Lässer, C. Detailed Analysis of the Plasma Extracellular Vesicle Proteome after
751 Separation from Lipoproteins. *Cell. Mol. Life Sci.* **2018**, *75*, 2873–2886, doi:10.1007/s00018-
752 018-2773-4.
753 14. Wei, R.; Zhao, L.; Kong, G.; Liu, X.; Zhu, S.; Zhang, S.; Min, L. Combination of Size-Exclusion
754 Chromatography and Ultracentrifugation Improves the Proteomic Profiling of Plasma-Derived
755 Small Extracellular Vesicles. *Biol. Proced. Online* **2020**, *22*, 12, doi:10.1186/s12575-020-00125-
756 5.
757 15. Driedonks, T.A.P.; Mol, S.; de Bruin, S.; Peters, A.-L.; Zhang, X.; Lindenbergh, M.F.S.; Beuger,
758 B.M.; van Stalborch, A.-M.D.; Spaan, T.; de Jong, E.C.; et al. Y-RNA Subtype Ratios in Plasma

759 Extracellular Vesicles Are Cell Type- Specific and Are Candidate Biomarkers for Inflammatory
760 Diseases. *J. Extracell. Vesicles* **2020**, *9*, 1764213, doi:10.1080/20013078.2020.1764213.
761 16. Zhang, L.; Song, J.; Cavigiolio, G.; Ishida, B.Y.; Zhang, S.; Kane, J.P.; Weisgraber, K.H.; Oda, M.N.;
762 Rye, K.-A.; Pownall, H.J.; et al. Morphology and Structure of Lipoproteins Revealed by an
763 Optimized Negative-Staining Protocol of Electron Microscopy. *J. Lipid Res.* **2011**, *52*, 175–184,
764 doi:10.1194/jlr.D010959.
765 17. Onódi, Z.; Pelyhe, C.; Terézia Nagy, C.; Brenner, G.B.; Almási, L.; Kittel, Á.; Manček-Keber, M.;
766 Ferdinandy, P.; Buzás, E.I.; Giricz, Z. Isolation of High-Purity Extracellular Vesicles by the
767 Combination of Iodixanol Density Gradient Ultracentrifugation and Bind-Elute Chromatography
768 From Blood Plasma. *Front. Physiol.* **2018**, *9*, doi:10.3389/fphys.2018.01479.
769 18. Wiklander, O.P.B.; Bostancioglu, R.B.; Welsh, J.A.; Zickler, A.M.; Murke, F.; Corso, G.; Felldin, U.;
770 Hagey, D.W.; Evertsson, B.; Liang, X.-M.; et al. Systematic Methodological Evaluation of a
771 Multiplex Bead-Based Flow Cytometry Assay for Detection of Extracellular Vesicle Surface
772 Signatures. *Front. Immunol.* **2018**, *9*, doi:10.3389/fimmu.2018.01326.
773 19. Menezes-Neto, A. de; Sáez, M.J.F.; Lozano-Ramos, I.; Segui-Barber, J.; Martin-Jaular, L.; Ullate,
774 J.M.E.; Fernandez-Becerra, C.; Borrás, F.E.; Portillo, H.A. del Size-Exclusion Chromatography as
775 a Stand-Alone Methodology Identifies Novel Markers in Mass Spectrometry Analyses of
776 Plasma-Derived Vesicles from Healthy Individuals. *J. Extracell. Vesicles* **2015**, *4*, 27378,
777 doi:10.3402/jev.v4.27378.
778 20. Looze, C.; Yui, D.; Leung, L.; Ingham, M.; Kaler, M.; Yao, X.; Wu, W.W.; Shen, R.-F.; Daniels,
779 M.P.; Levine, S.J. Proteomic Profiling of Human Plasma Exosomes Identifies PPARγ as an
780 Exosome-Associated Protein. *Biochem. Biophys. Res. Commun.* **2009**, *378*, 433–438,
781 doi:10.1016/j.bbrc.2008.11.050.
782 21. Karimi, N.; Dalirfardouei, R.; Dias, T.; Lötvall, J.; Lässer, C. Tetraspanins Distinguish Separate
783 Extracellular Vesicle Subpopulations in Human Serum and Plasma – Contributions of Platelet
784 Extracellular Vesicles in Plasma Samples. *J. Extracell. Vesicles* **2022**, *11*, e12213,
785 doi:10.1002/jev2.12213.
786 22. Graham, J. OptiPrep™ Density Gradient Solutions for Mammalian Organelles. *Sci. World J.*
787 **2002**, *2*, 1440–1443, doi:10.1100/tsw.2002.840.
788 23. Schneider, C.A.; Rasband, W.S.; Eliceiri, K.W. NIH Image to ImageJ: 25 Years of Image Analysis.
789 *Nat. Methods* **2012**, *9*, 671–675, doi:10.1038/nmeth.2089.
790 24. Verleysen, E.; Wagner, T.; Lipinski, H.-G.; Kägi, R.; Koeber, R.; Boix-Sanfeliu, A.; De Temmerman,
791 P.-J.; Mast, J. Evaluation of a TEM Based Approach for Size Measurement of Particulate
792 (Nano)Materials. *Materials* **2019**, *12*, 2274, doi:10.3390/ma12142274.
793 25. Lige, T.; Liguo Wang Cryo-EM Sample Preparation Method for Extremely Low Concentration
794 Liposomes. *Ultramicroscopy* **2020**, *208*, 112849, doi:10.1016/j.ultramic.2019.112849.
795 26. Van Deun, J.; Mestdagh, P.; Agostinis, P.; Akay, Ö.; Anand, S.; Anckaert, J.; Martinez, Z.A.;
796 Baetens, T.; Beghein, E.; Bertier, L.; et al. EV-TRACK: Transparent Reporting and Centralizing
797 Knowledge in Extracellular Vesicle Research. *Nat. Methods* **2017**, *14*, 228–232,
798 doi:10.1038/nmeth.4185.
799

800

801 **Main Figures:**

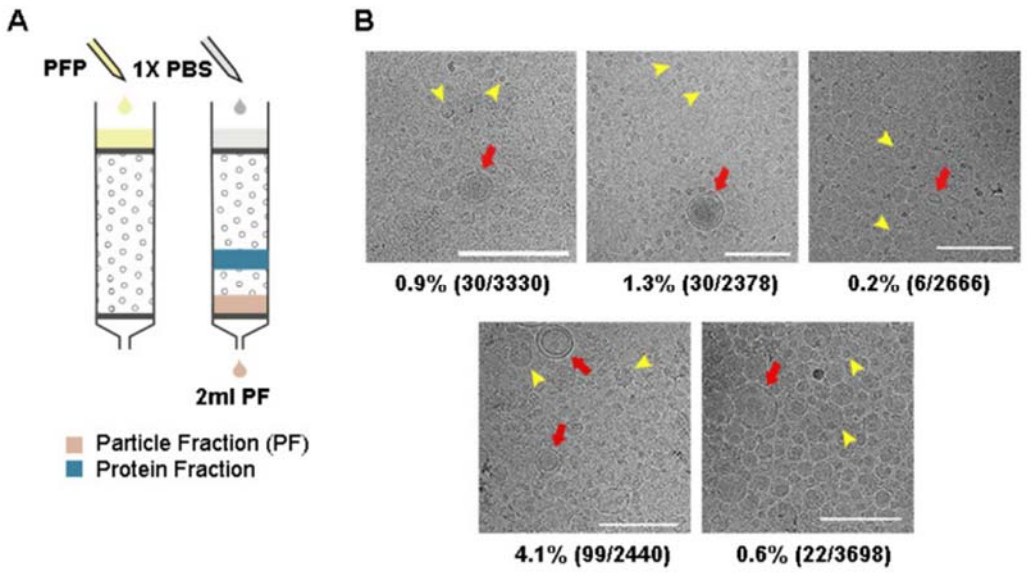

802

803 **Figure 1: SEC was effective in removing plasma proteins and HDL but not low-density lipoproteins**.
804 (A) 500 *µl* of plasma was loaded on a SEC column and PFs were collected. (B) Cryo-EM images of PFs
805 obtained from the plasma of 5 healthy individuals. Vesicles could be easily identified and the images
806 revealed a clean background suggesting minimum protein contamination. Moreover, HDL was sparse
807 in the Cryo-EM images, indicating that they were also largely removed. Furthermore, sEVs, having
808 clearly defined bilayer (red arrows), were easily distinguishable from lipoproteins (representative
809 particles marked by yellow arrows). The ratio of counted sEVs to all vesicles are shown under each
810 image. All scale bars represent 200 *nm*.

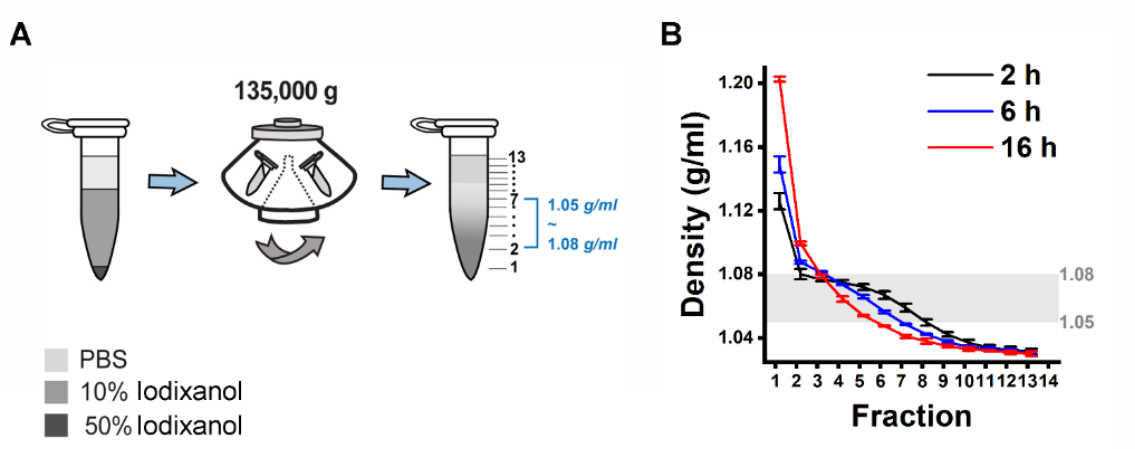

811

812 **Figure 2: Design of a density gradient setup in a small volume format.** (A) 500 *µl* PBS was overlaid on
813 800 *µl* 10% iodixanol solution and 20 *µl* 50% iodixanol cushion. The 1.5 *ml* tubes were subjected to
814 ultracentrifugation using a fixed-angle rotor at an average speed of 135,000 *g* for 2, 6 and 16 *h* at 4 *°C*
815 to establish a density gradient profile. (B) Density gradient profiles along the 1.5 *ml* tubes after
816 ultracentrifugation. The 2 *h* spinning time gave a density profile with the largest separation zone of
817 1.05~1.08 *g/ml* and smallest sEV zone of >1.08 *g/ml*. The data shows the average ± standard deviation
818 of 7 repeats for 2 *h*, 3 repeats each for 6 and 16 *h*.

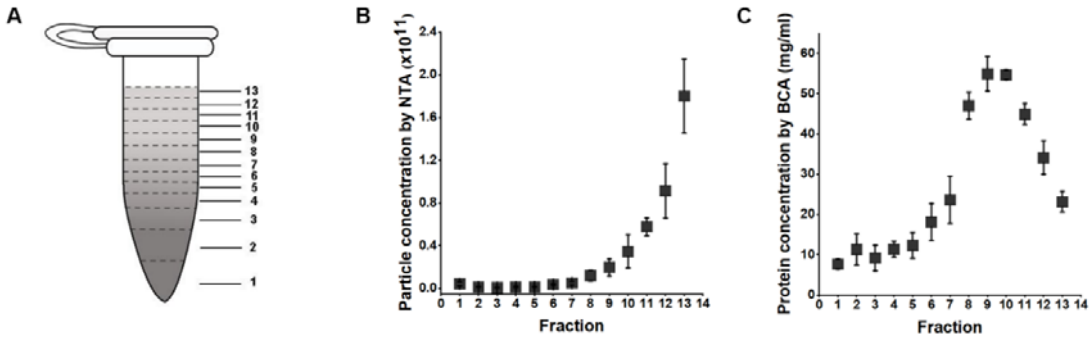

Figure 3: Particle and protein concentrations along the 1.5 *ml* tube after applying DGUC to plasma. (A) The 1.5 ml tube was fractionated into 13 fractions. (B) Particle concentration ± std measured by NTA of different fractions (n=3). (C) Protein concentrations ± std measured by BCA of different fractions (n=3).

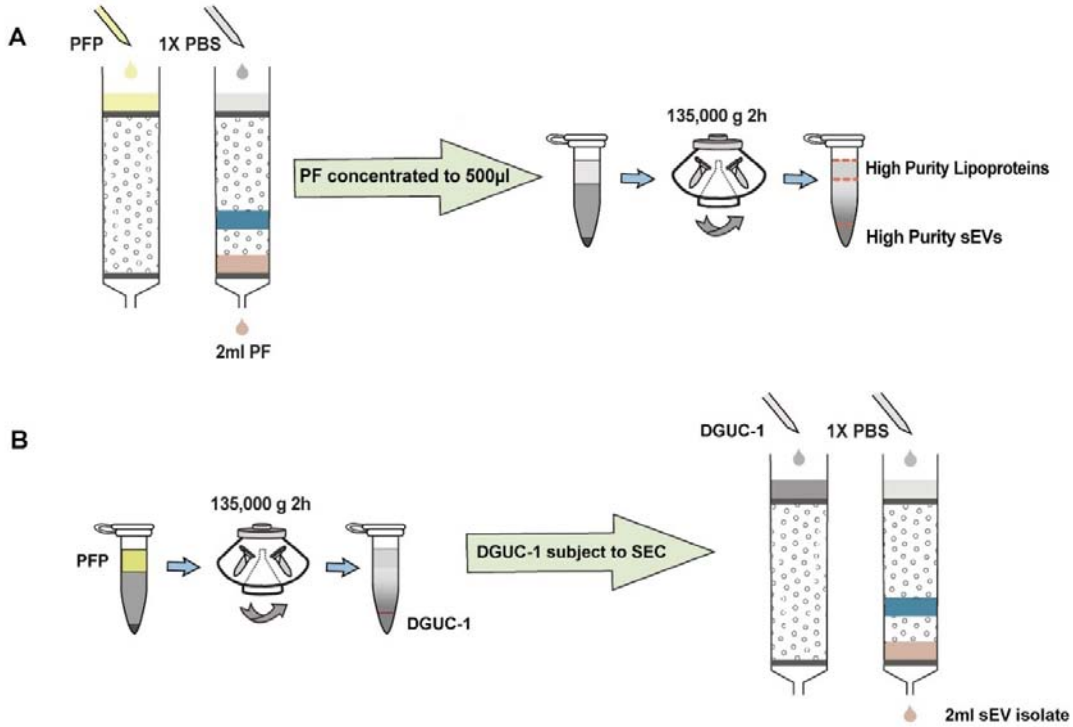

Figure 4: Schematic representation of the SEC-DGUC and DGUC-SEC protocols. (A) Illustrates the SEC-DGUC protocol sequence. Starting from the left, SEC is used initially to separate plasma proteins and HDL. Subsequently, DGUC is employed to separate low-density lipoproteins (i.e., IDL, VLDL, LDL) from sEVs. (B) Depicts the DGUC-SEC protocol, wherein DGUC is initially employed to segregate high-density components from those of lower density, before SEC is applied to partition any remaining proteins from the sEVs.

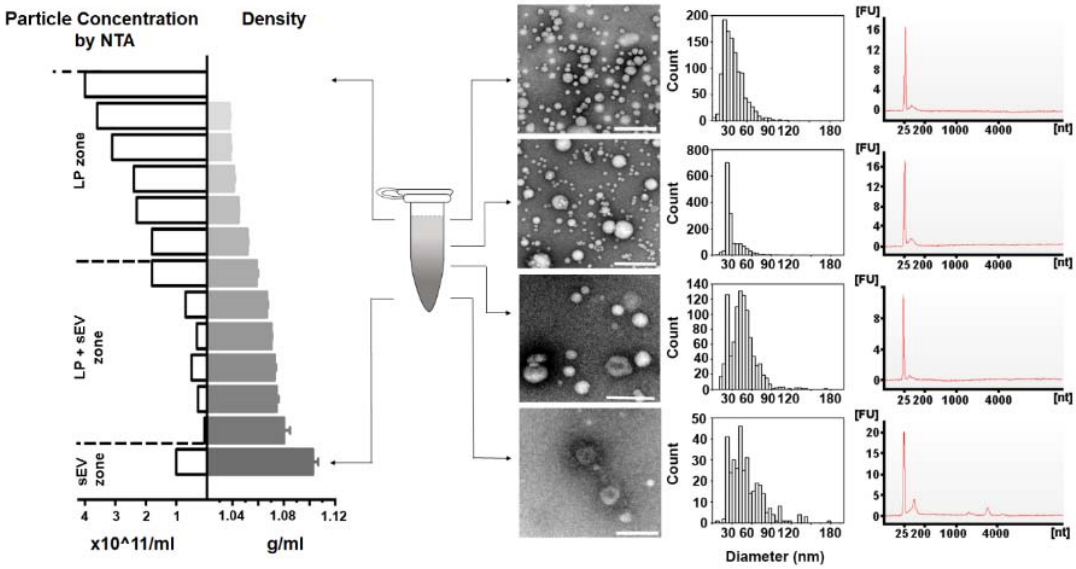

Figure 5: DGUC in the 1.5 *ml* tube format effectively separated sEVs from lipoproteins. PFs obtained from SEC were concentrated into 500 *µl*, loaded onto the density gradient and subjected to ultracentrifugation as previously described. After DGUC, the 1.5 *ml* tube was fractionated into 13 fractions, which were each examined for their particle concentration (by NTA) and the presence of sEVs and lipoproteins (by TEM). In the sEV zone (bottom of the tube), where density was higher than 1.08 *g/ml*, high purity sEVs were indeed observed. A mixed population of sEVs and lipoproteins was observed within the density zone of 1.05~1.08 *g/ml*. Interestingly, the particle numbers in this density zone were low, thus creating an effective separation zone between lipoproteins and sEVs. The RNA profiles of corresponding particle populations are shown on the right. All scale bars represent 200 *nm*.

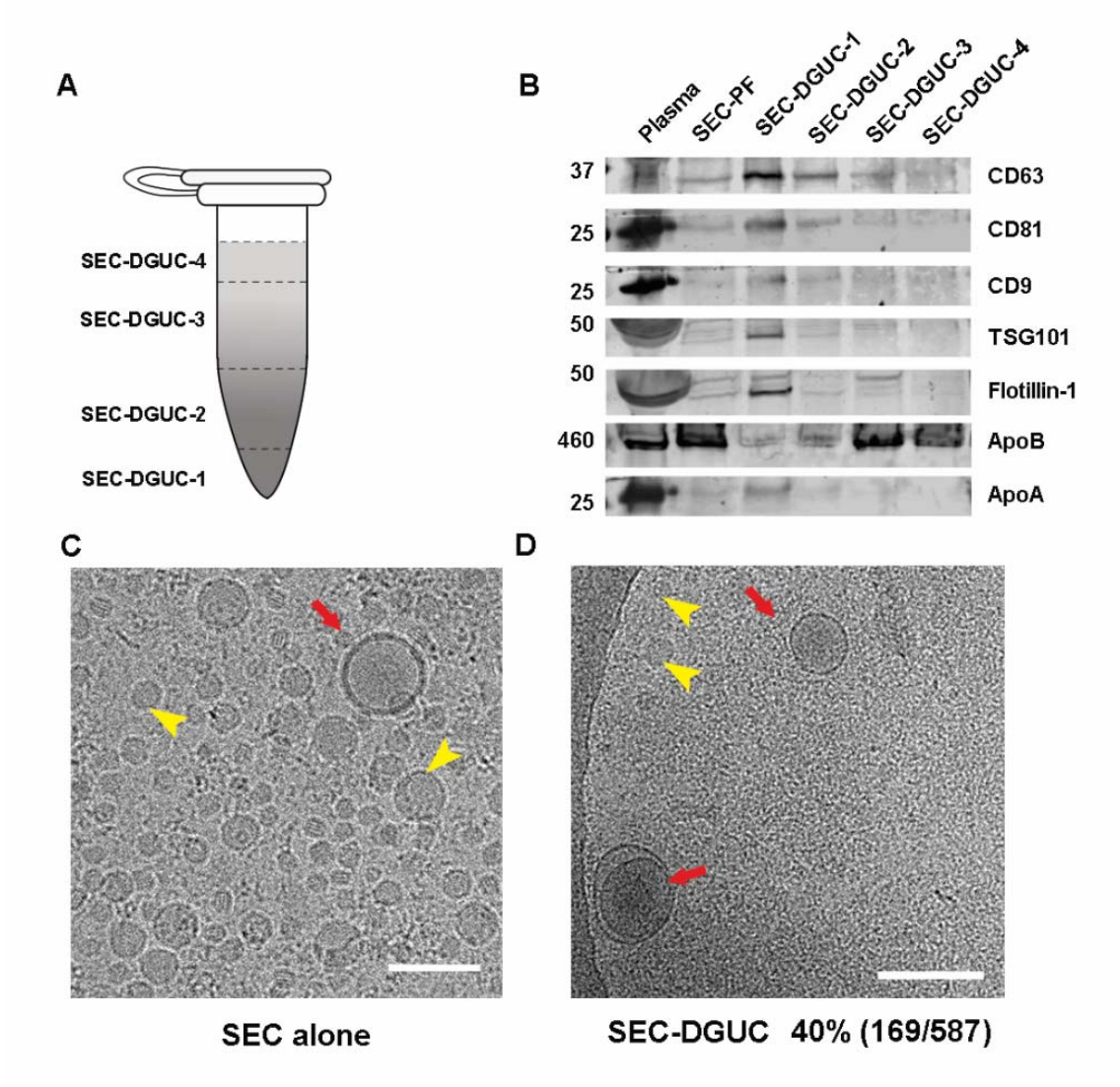

Figure 6: The high purity of sEVs in SEC-DGUC-1 was demonstrated by WB and Cryo-EM. (A) The 1.5 *ml* tube subjected to the SEC-DGUC protocol was fractionated into 4 fractions for easier analysis. (B) Western blot analyses of original plasma, SEC-PF, SEC-DGUC-1 to 4 using sEV and lipoprotein markers. (C) & (D) Cryo-EM images showing the comparison between SEC-PF and SEC-DGUC-1. The SEC-DGUC-1 in (D) was obtained from non-fasting plasma collected in EDTA tubes. All scale bars represent 200 *nm*.

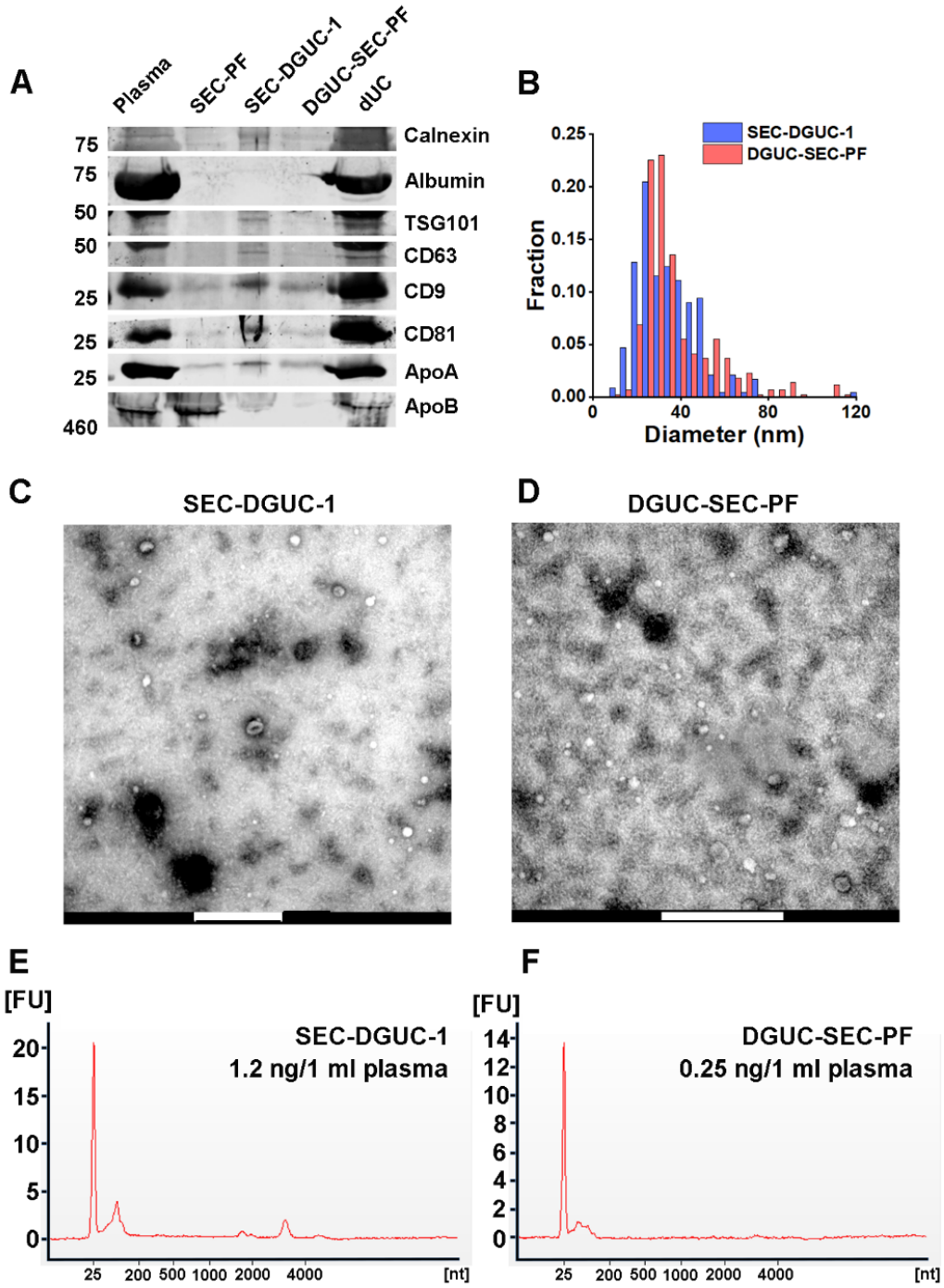

Figure 7: Comparison of sEVs isolated by SEC-DGUC and DGUC-SEC protocols. (A) Western blot of SEC-DGUC-1, DGUC-SEC-PF, sEV isolated by dUC obtained from 2 *ml* of plasma of the same source. (B) Particle size distributions in SEC-DGUC-1 and DGUC-SEC-PF measured by TEM. (C) and (D) TEM images of SEC-DGUC-1 and DGUC-SEC-PF. (E) and (F) Total RNA analyses of SEC-DGUC-1 and DGUC-SEC-PF. Note that data in (E) is the same data shown in the bottom right subfigure of Figure 5.

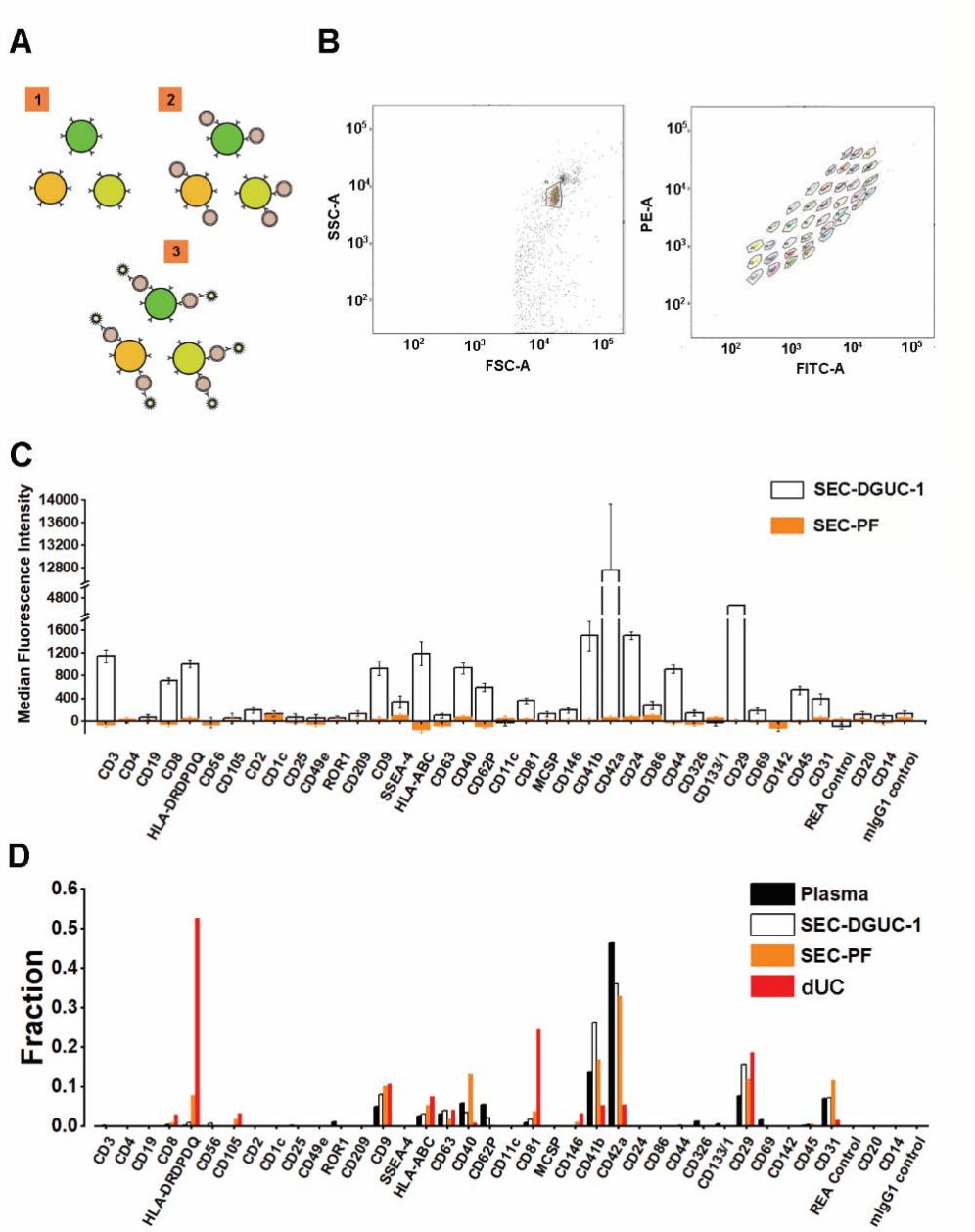

Figure 8: Flow cytometry assay using MACSPlex exosome kit to evaluate sEV isolates. (A) Illustration of the principle of MACSPlex exosome kit. 37 types of beads with different fluorescent colors are functionalized with specific antibodies against sEV surface proteins. sEVs captured by the beads are detected with flow cytometry using APC labeled anti-CD9, CD63, CD81 antibodies. (B) Flow cytometry gating setup. (C) A representative data showing the comparison of median fluorescence intensity (MFI) ± standard error of the mean (SEM) from sEV isolates obtained from SEC-PF and SEC-DGUC-1. Equal numbers of particles ($5x10^8$, based on NTA) were loaded for both samples. (D) Comparison of signal patterns among plasma, SEC-DGUC-1, SEC-PF and dUC. The Results showed that sEVs isolated from dUC deviate from plasma whereas, sEVs in the SEC-PF and SEC-DGUC-1 mirror the sEV population in plasma.

870

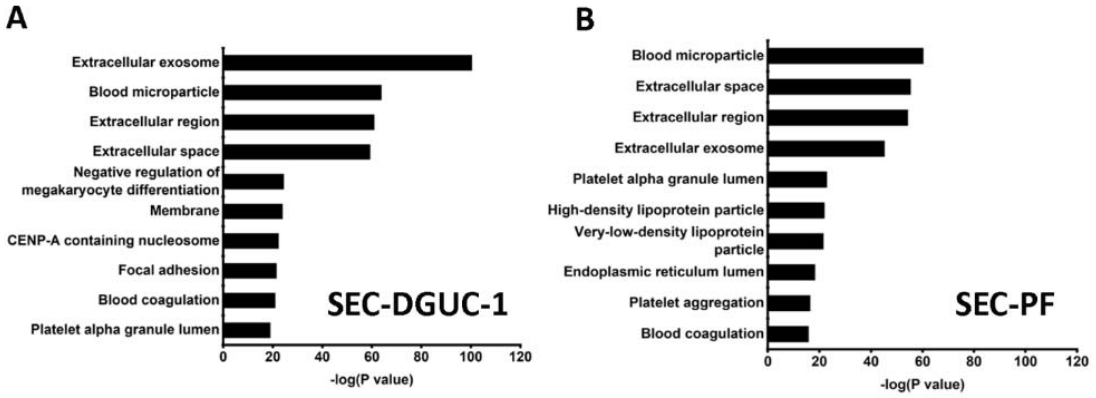

871

872 **Figure 9: Functional annotation of proteins identified by LC-MS/MS.** (A) Functional annotation of
873 proteins identified in SEC-DGUC-1. (B) Functional annotation of proteins identified in SEC-PF.

874

875

876

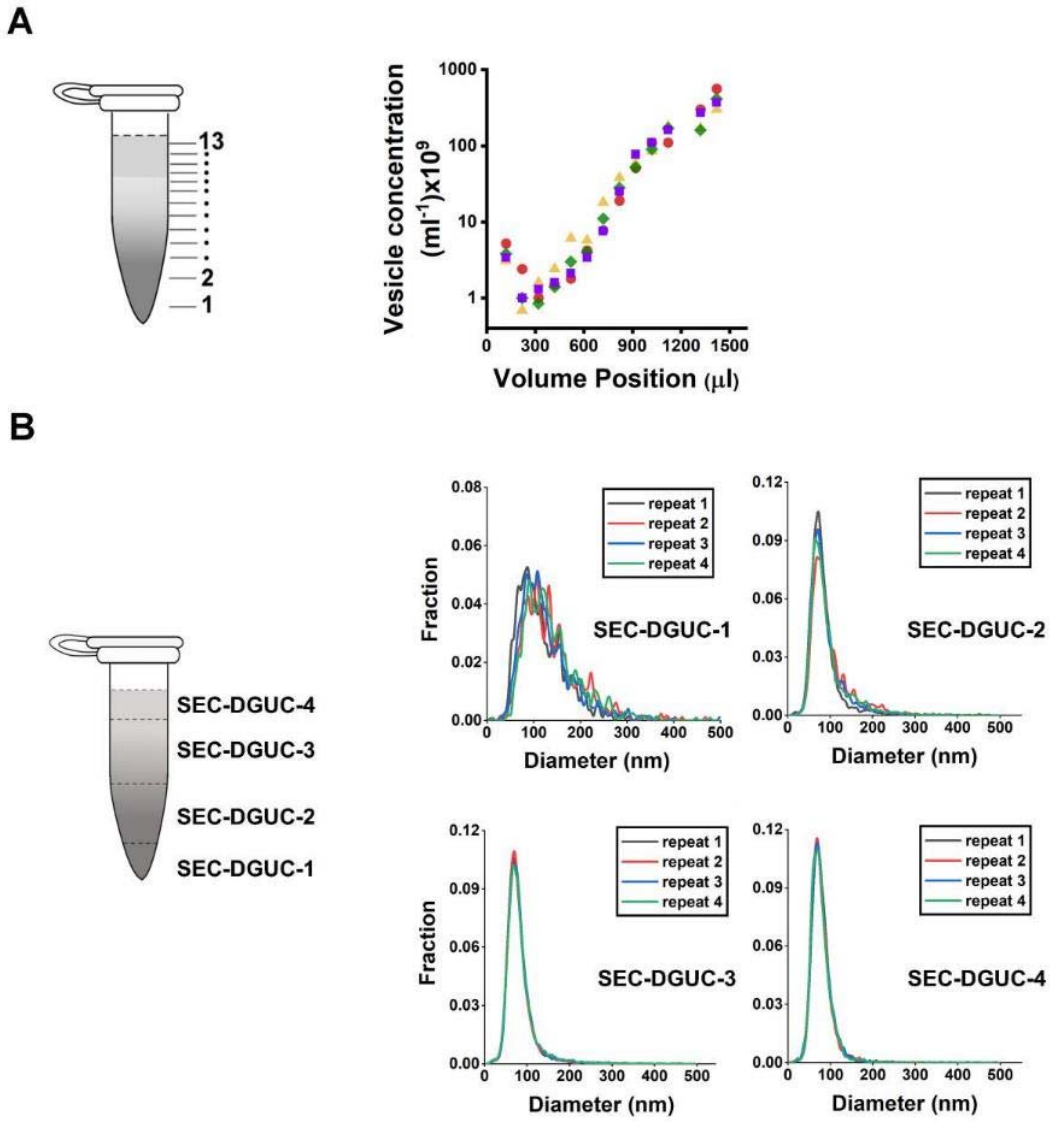

Figure 10: Repeatability of the SEC-DGUC protocol. (A) Particle concentration profiles (by NTA) along the 1.5 *ml* tube from 4 technical replicates subjected to SEC-DGUC protocol. (B) Particle size distributions measured by NTA in the four fractions indicated on the left figure. Four technical replicates subjected to SEC-DGUC protocol were shown.

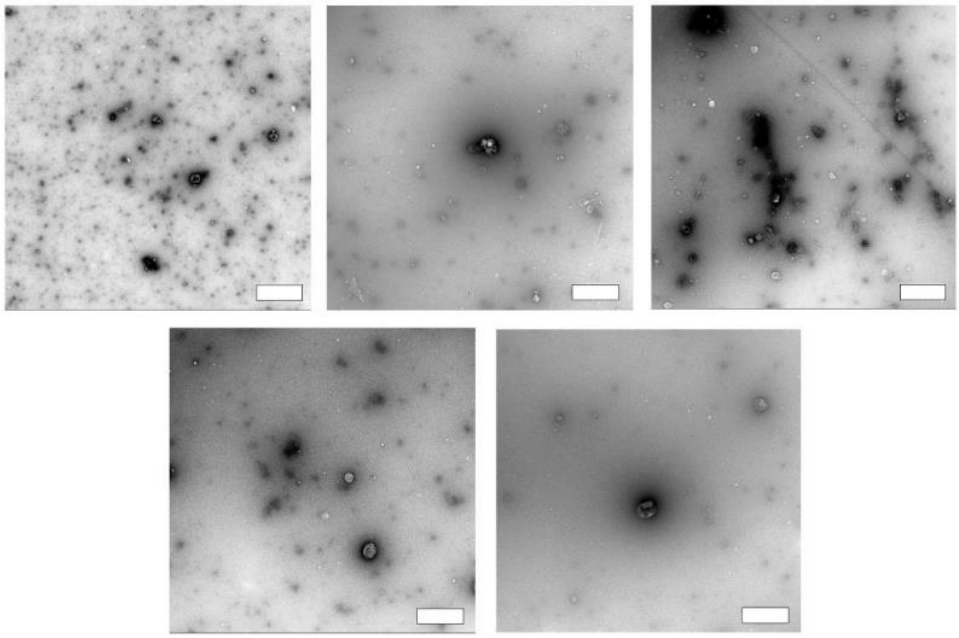

882

883 **Figure 11: Reliability of the SEC-DGUC protocol.** TEM images of SEC-DGUC-1 were obtained from 5
884 fasting plasma (Biobank samples, EDTA tubes). High purity of sEVs represented by the low-contrast,
885 cup-shaped vesicles was evident across different samples, suggesting the SEC-DGUC was reliable in
886 obtaining high-purity sEVs. All scale bars represent 200 *nm.*

887

888

889

Plasma	SEC-PF	SEC-DGUC-1
$8x10^{10}$	$6.5x10^{10}$	$1.8x10^{9}$
$5.5x10^{11}$	$1.65x10^{11}$	$1.32x10^{9}$
$1.75x10^{11}$	$8.5x10^{10}$	$1.68x10^{9}$
$6x10^{11}$	$1.2x10^{11}$	$1.56x10^{9}$
$2.4x10^{10}$	$1.6x10^{10}$	$1.2x10^{9}$

890

891 **Table I. Particle numbers in different steps during the SEC-DGUC protocol, calculated based on NTA**
892 **measurement.** The first column provides the total particle numbers measured in 500 *µl* fasting plasma
893 (~1 *ml* of whole blood) from 5 individuals. The second column provides the corresponding total vesicle
894 numbers in SEC-PF after the plasma was subjected to SEC. The third column provides the
895 corresponding total vesicle numbers in SEC-DGUC-1 after the SEC-PF was subjected to DGUC.
896

897 **Supplementary Figure Data:**

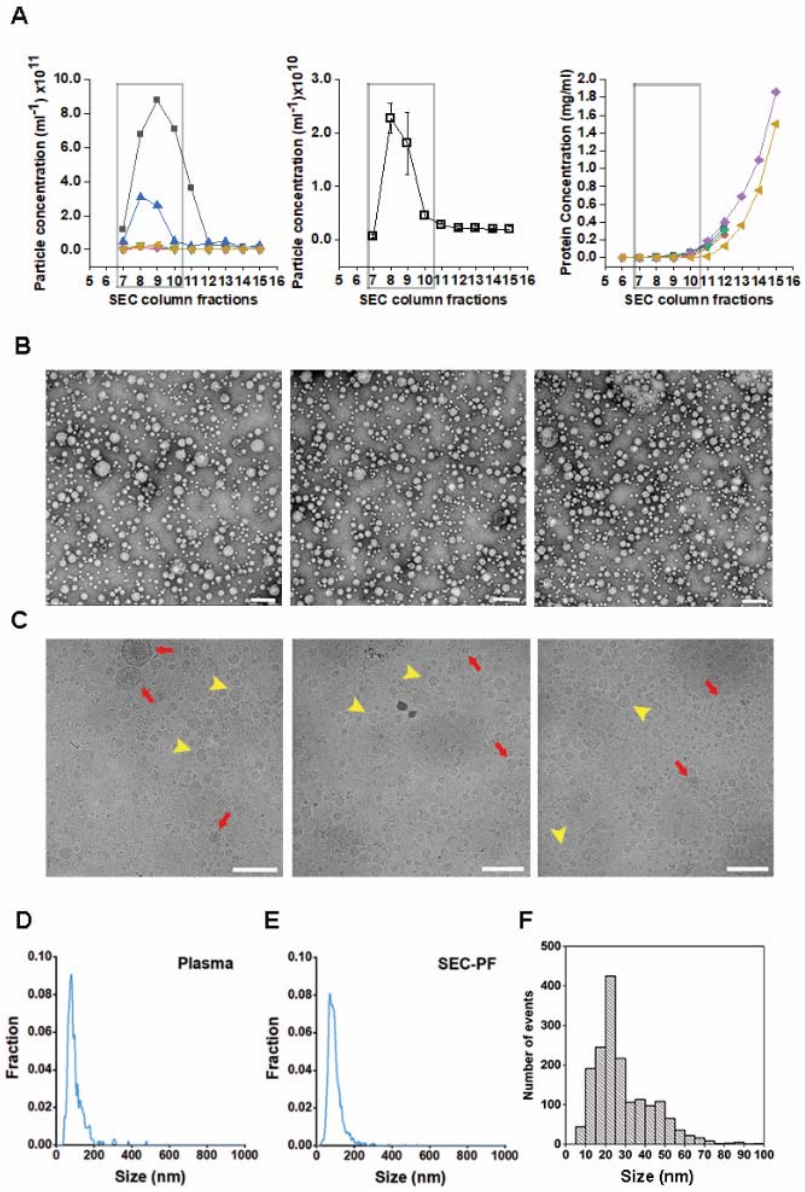

898

899 **Supplementary Figure 1: SEC elution profiles, EM images of the PF and particle size distributions.** (A)
900 SEC elution profiles according to particle concentration (by NTA) of 6 different plasma sources (left)
901 and 4 repeats of the same plasma source (middle). Protein concentrations (by BCA, right) in
902 corresponding to the elution profiles of the 6 different plasma sources shown on the left. 500 μl of
903 plasma was loaded onto the SEC column and 10 fractions of 500 μl each were collected and analyzed.
904 Fraction 7 to 10 were pooled to constitute the SEC-PF because of their high particle concentrations
905 and low protein concentrations. (B) Representative TEM images of the PF. (C) Cryo-EM images of the
906 SEC-PF. (D), (E) Typical particle size distributions of a plasma and SEC-PF measured by NTA. (E) A
907 histogram of particle diameter obtained from the TEM images shown in (B).
908

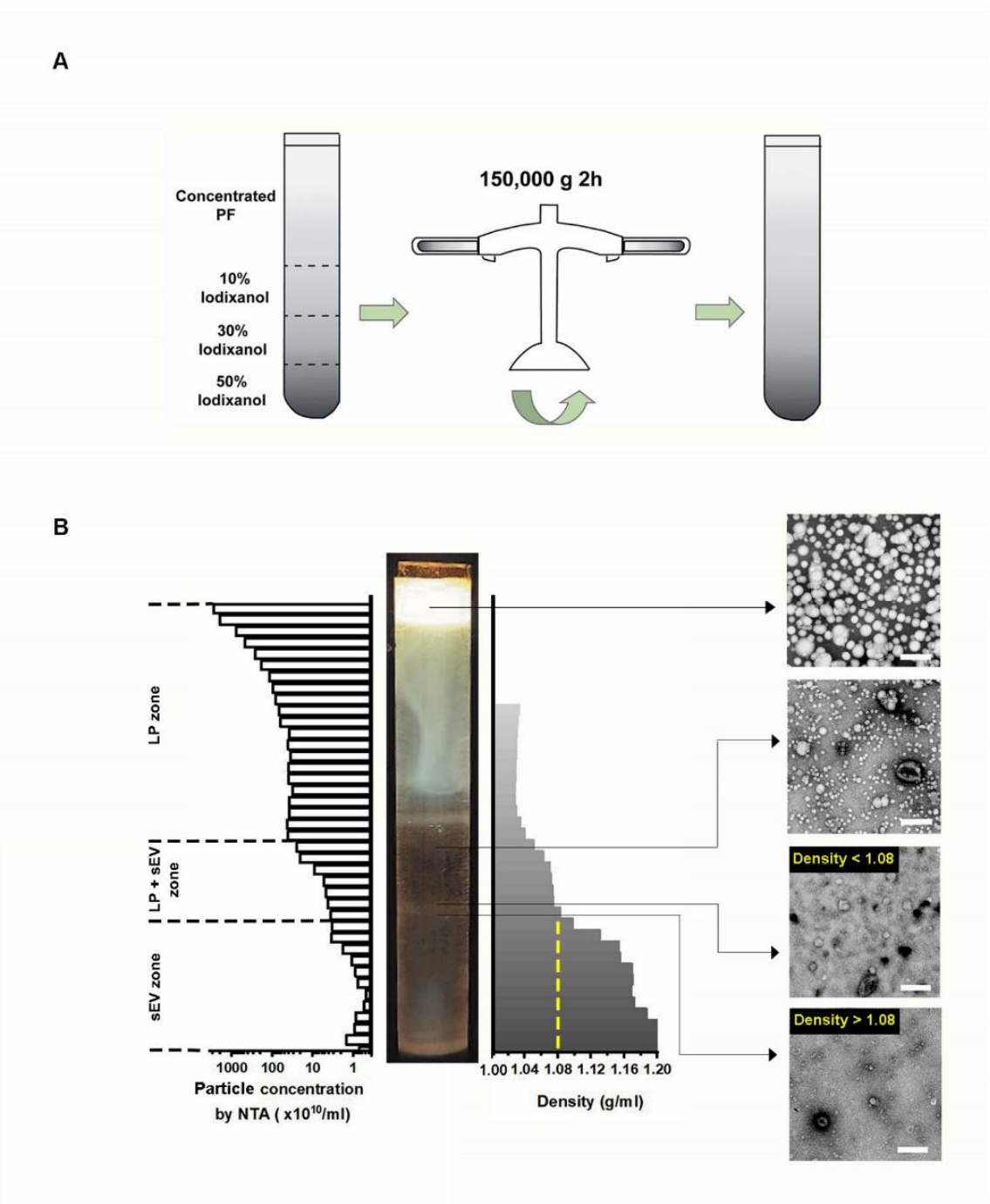

Supplementary Figure 2: Distribution of sEVs and lipoproteins within the density gradient after DGUC. (A) SEC-PFs (6 *ml*) were placed on top of a density gradient cushion constructed with 2 *ml* 10%, 2 *ml* 30%, and 2 *ml* 50% iodixanol solutions and centrifuged at 150,000 x *g* for 2 *h* at 4 *°C*. (B) After DGUC, the tube was fractionated into 42 fractions, which were each examined for their densities, particle concentrations (by NTA) and presence of sEVs and lipoproteins (by TEM). The dominance of lipoproteins was evident in fractions of density <1.05 *g/ml,* which is designated as LP zone. sEVs started to appear when density exceeded 1.05 *g/ml* but a significant level of lipoproteins was present until the density of 1.08 *g/ml*. Therefore, the density region of 1.05~1.08 *g/ml* was designated as

LP+sEV zone. Beyond 1.08 *g/ml*, lipoproteins diminished drastically and the density region of >1.08 *g/ml* was designated as the sEV zone. All scale bars represent 200 *nm*.

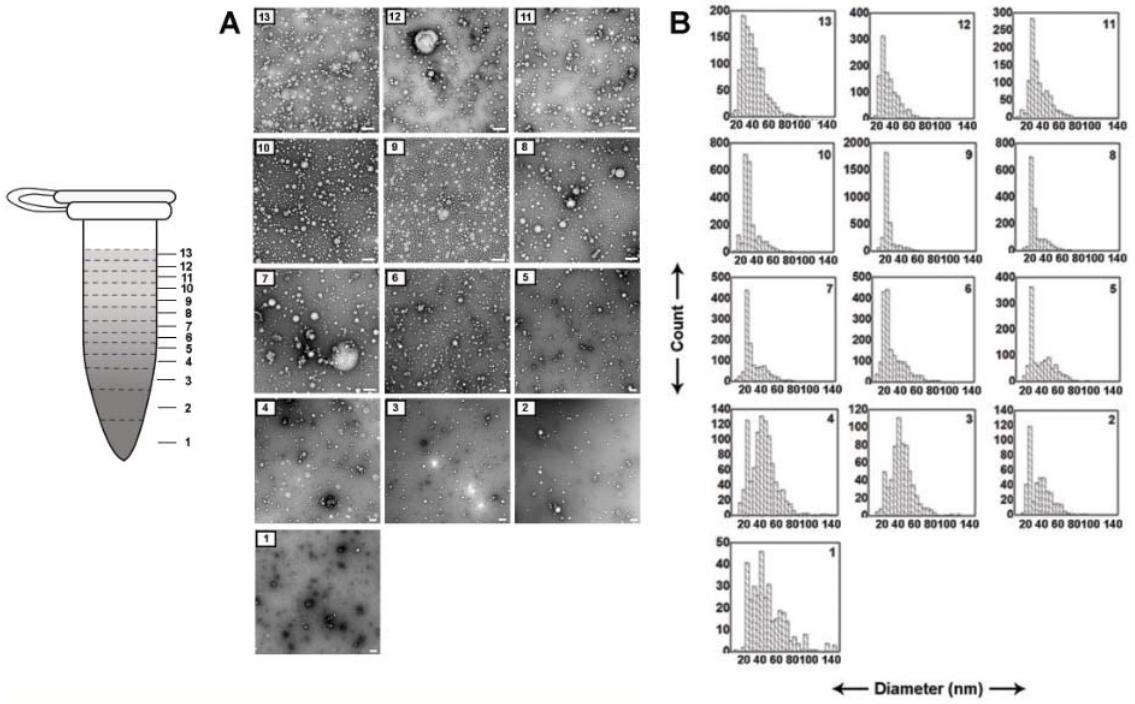

Supplementary Figure 3: TEM images and size distributions of the 13 fractions collected from the 1.5 *ml* tube following SEC-DGUC. (A) Representative TEM images of each of the 13 fractions. SEC-DGUC-1 clearly showed minimum presence of lipoprotein (high contrast lighter color particles) compared to other fractions. Moreover, the presence of sEVs (low contrast and cup-shaped particles) is evident in SEC-DGUC-1. (B) Particle size distributions measured according to the TEM images of the 13 fractions. Note the differences in the particle size distributions obtained from NTA measurement and TEM.

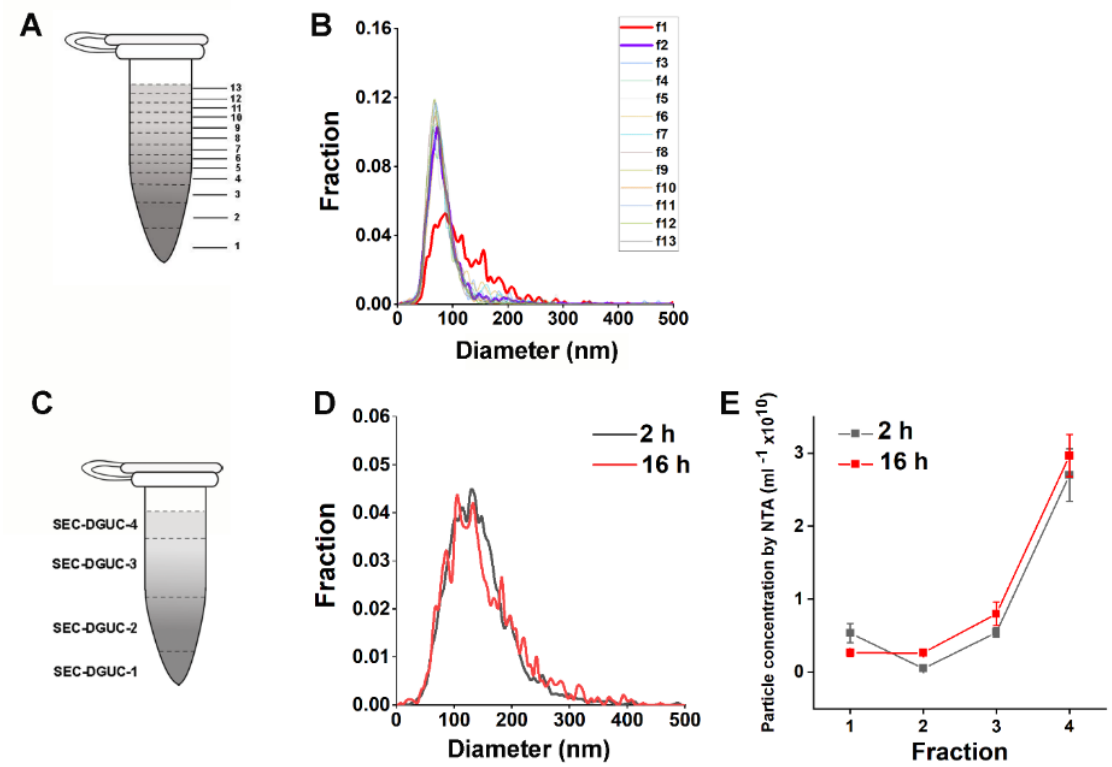

930

931 **Supplementary Figure 4:** (A) The 1.5 ml tube was fractionated into 13 fractions. (B) Size distributions
932 (by NTA) of the 13 fractions collected from the 1.5 *ml* tube following SEC-DGUC protocol. The particle
933 size distribution in SEC-DGUC-1 was distinct from the rest of the fractions. Even in SEC-DGUC-2
934 (highlighted in purple), the size distribution follows fractions 3~13, implying the dominance of
935 lipoproteins in these fractions. (C) The 1.5 *ml* tube was fractionated into 4 fractions in order to examine
936 if 2 *h* spinning time was sufficient to isolate sEV from lipoproteins in the 1.5 *ml* tube format DGUC. (D)
937 The resulting size distributions of SEC-DGUC-1s (by NTA) were highly similar for 2 *h* and 16 *h* spinning
938 time. (E) The particle concentrations of the four individual fractions along the 1.5 *ml* tube closely
939 resembled each other for 2 *h* and 16 *h*, implying that there were no significant loss of sEV for 2 *h*
940 spinning time in comparison to 16 *h*.

941

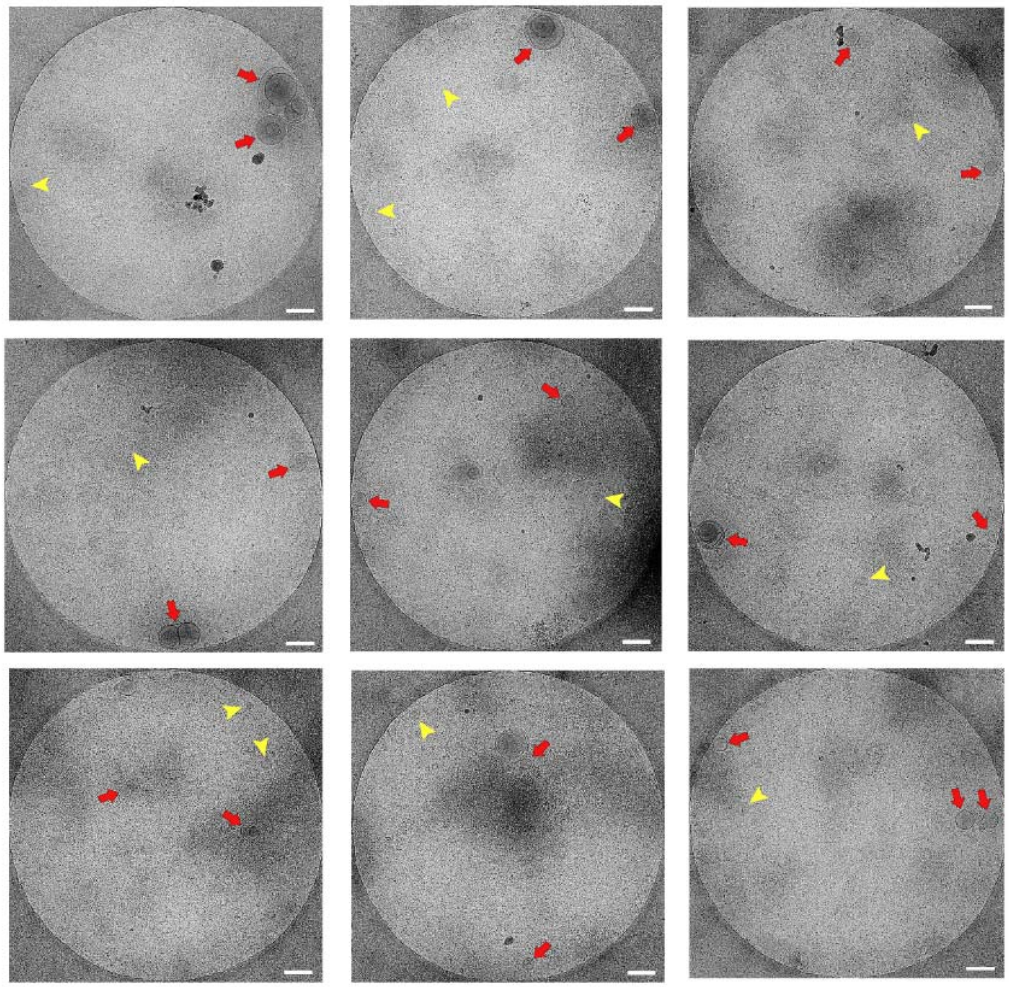

942

943 **Supplementary Figure 5: Additional Cryo-EM images of SEC-DGUC-1.** Red arrows represent sEVs and
944 yellow arrows represent typical lipoproteins. The SEC-DGUC-1 was obtained from non-fasting plasma
945 collected in EDTA tubes. All scale bars represent 200 *nm*.

946

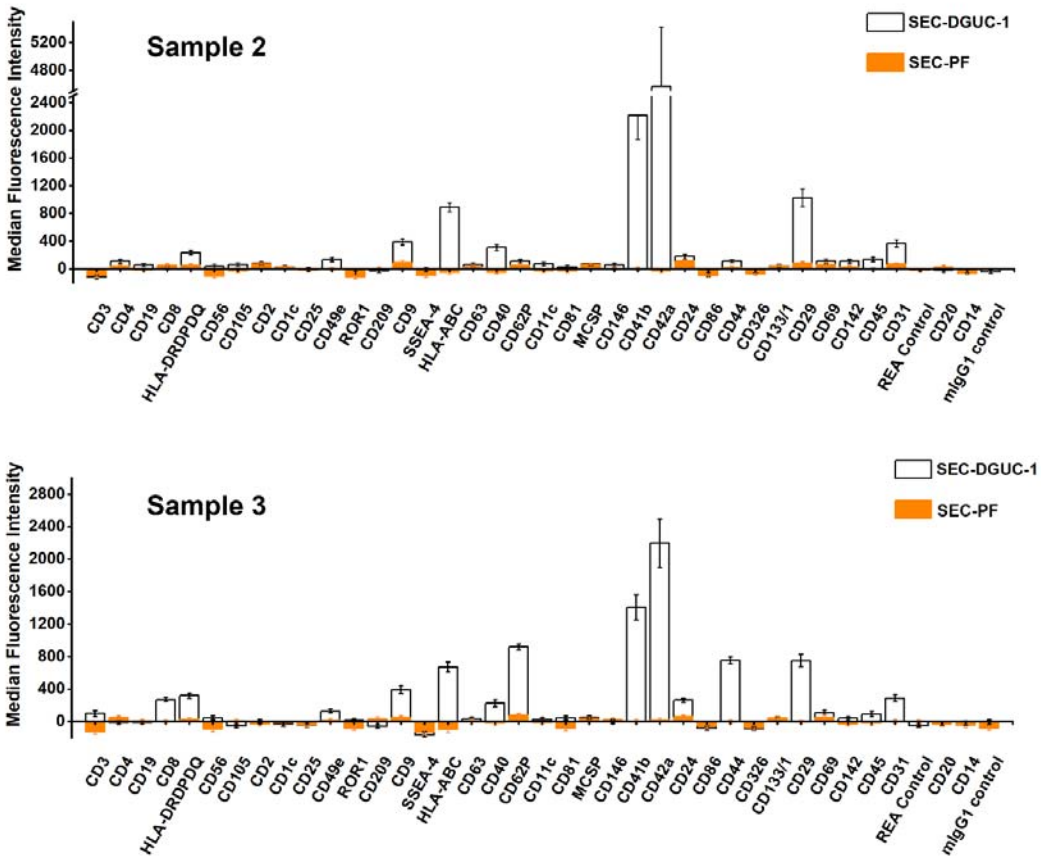

Supplementary Figure 6: Flow cytometry data of SEC-PF vs. SEC-DGUC-1 obtained from two plasma sources using MACSPlex exosome kit. Data from two plasma sources demonstrated a similar trend of much stronger signals of SEC-DGUC-1 compared to SEC-PF in flow cytometry using MACSPlex exosome kit. Data are Median ± SEM.

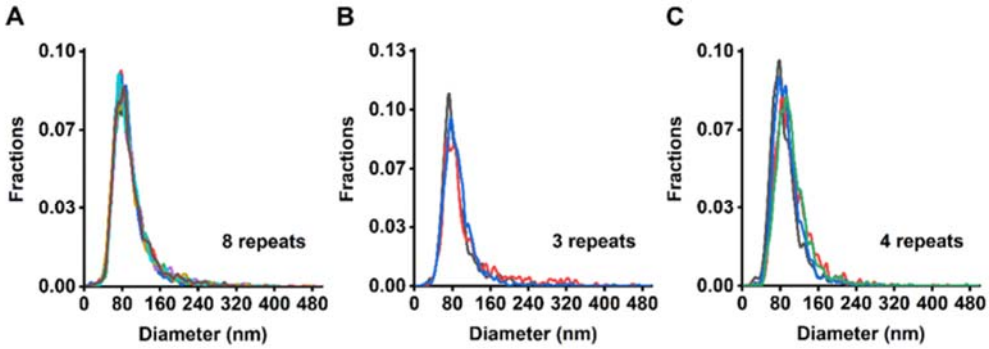

Figure number	Average vesicle concentration	Standard Deviation	SD/average ratio	Number of measurements
A	$1.6x10^{12}$	$4.2x10^{11}$	26%	8
B	$3.1x10^{11}$	$9.3x10^{10}$	30%	3
C	$2.2x10^{11}$	$1.2x10^{11}$	55%	4
	$8.6x10^{10}$	$2.9x10^{10}$	33%	3
	$4.7x10^{11}$	$2.8x10^{10}$	6%	3
	$9.6x10^{9}$	$7.0x10^{8}$	7%	3

Supplementary Figure 7: Repeatability of SEC. (A-C) Particles size distributions of SEC-PF measured by NTA. (A), (B) and (C) correspond to the first, second and third rows of the table, respectively. The highly overlapped size distributions allude to the consistency in the particles eluted from SEC columns, even though the number of particles eluted varied up to 55%. The table lists six experiments with various numbers of repeats of SEC. The average particle concentrations, standard deviation and CV (SD/average ratio) are listed together with the number of measurements made.

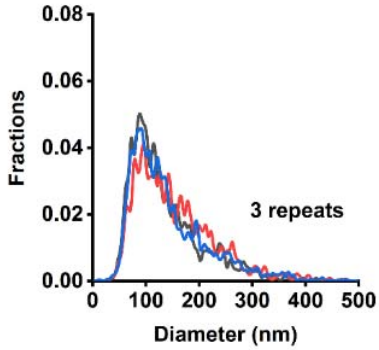

Average vesicle concentration	Standard Deviation	SD/average ratio	Number of measurements
$3.9x10^{9}$	$9.3x10^{8}$	24%	4
$2.0x10^{10}$	$5.0x10^{9}$	25%	3

Supplementary Figure 8: Repeatability of SEC-DGUC protocol. NTA measurements of two experiments to test repeatability after SEC-DGUC. The figure displays the size distributions measured by NTA of the experiment listed in the second row of the table. The size distributions of the experiment

963 listed in the first row of the table were presented in main Figure 9. The table lists the average particle
964 concentrations of SEC-DGUC-1 and the standard deviation, CV (SD/average ratio) together with the
965 number of measurements made.

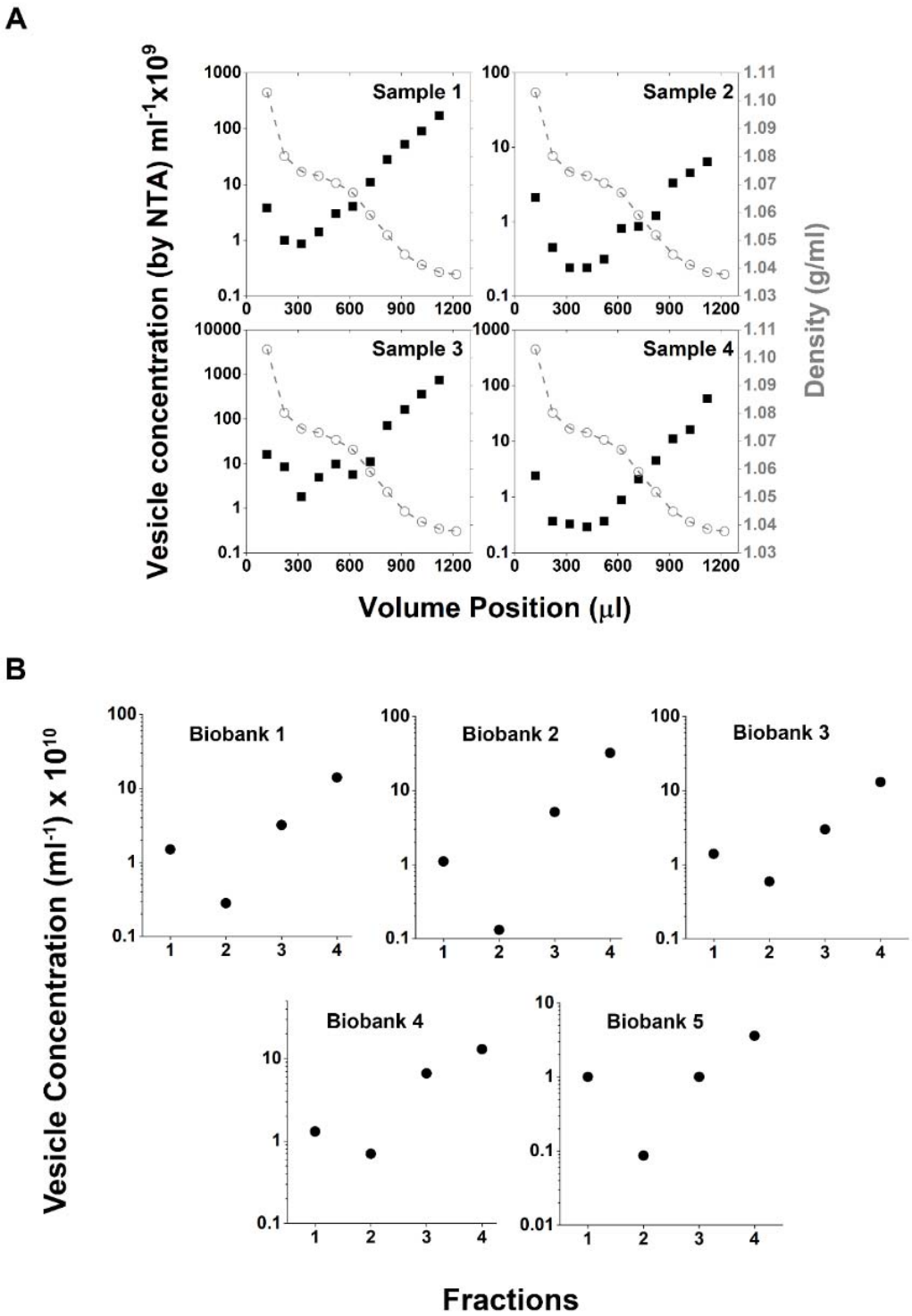

966

967 **Supplementary Figure 9: Reliability of particle concentration profiles along the 1.5 *ml* tube (by NTA).**
968 (A) Detailed particle concentration profiles (13 fractions) of four different samples along with the
969 calibrated density profile shown in Figure 2. (B) Five particle concentration profiles (4 fractions shown
970 in Figure 9B) in SEC-DGUC-1 corresponding to the biobank plasma samples (EDTA tubes) shown in
971 Figure 11. Note that the data from (A) and (B) are from different plasma sources.

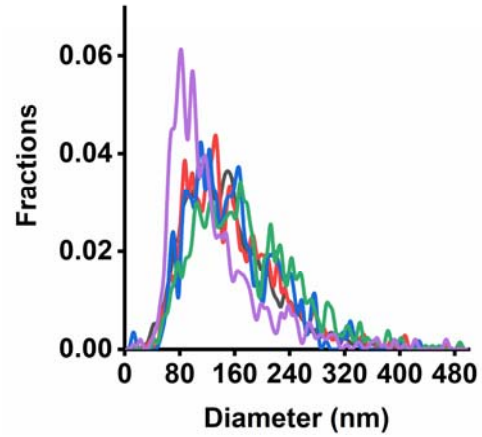

972

973 **Supplementary Figure 10: Size distributions (by NTA) of SEC-DGUC-1 obtained from 5 fasting plasma**
974 **corresponding to Figure 11.** The particle size distributions did not overlap, reflecting the variation of
975 sEV population among different plasma sources.

976